Impaired Myocardium Regeneration With Skeletal Cell Sheets—A Preclinical Trial for Tissue-Engineered Regeneration Therapy

Shigeru Miyagawa,[1] Atsuhiro Saito,[2] Taichi Sakaguchi,[1] Yasushi Yoshikawa,[1] Takashi Yamauchi,[1] Yukiko Imanishi,[1] Naomasa Kawaguchi,[3] Noboru Teramoto,[4] Nariaki Matsuura,[3] Hidehiro Iida,[4] Tatsuya Shimizu,[5] Teruo Okano,[5] and Yoshiki Sawa[1,6]

Background. We hypothesized that autologous skeletal cell (SC) sheets regenerate the infract myocardium in porcine heart as a preclinical trial.

Methods and Results. The impaired heart was created by implantation of ameroid constrictor on left anterior descending for 4 weeks. SCs isolated from leg muscle were cultured and detached from the temperature-responsive domain-coated dishes as single monolayer cell sheet at 20°C. The following therapies were conducted: SC sheets (SC group, n=5); sham (C group n=5). Echocardiography demonstrated that cardiac performance was significantly improved in the SC group 3 and 6 months after operation (fractional area shortening, 3 months; SC vs. C=49.5±2.8 vs. 24.6±2.0%, $P<0.05$) and left ventricle dilatation was well attenuated in the SC group. Color kinesis index showed that distressed regional diastolic and systolic function in infarcted anterior wall was significantly recovered (SC vs. C=57.4±8.6 vs. 30.2±4.7%, $P<0.05$, diastolic: 58.5±4.5 vs. 35.4±6.6%, $P<0.05$, systolic). Factor VIII immunostains demonstrated that vascular density was significantly higher in the SC group than the C group. And % fibrosis and cell diameter were significantly lower in the SC group. And hematoxylin-eosin staining depicted that skeletal origin cells and well-developed-layered smooth muscle cells were detected in the implanted area. Positron emission tomography showed better myocardial perfusion and more viable myocardial tissue in the distressed myocardium receiving SC sheets compared with the myocardium receiving no sheets.

Conclusions. SC sheet implantation improved cardiac function by attenuating the cardiac remodeling in the porcine ischemic myocardium, suggesting a promising strategy for myocardial regeneration therapy in the impaired myocardium.

Keywords: Cells, Heart failure, Myocardial infarction, Tissue, Transplantation.

(*Transplantation* 2010;90: 364–372)

Despite the recent remarkable progress in medical and surgical treatments for heart failure, end-stage heart failure has been still a major cause of death worldwide. After myocardial infarction, the myocardium is capable of a limited regenerative capacity and no medication or procedure used clinically has shown efficacy in regenerating myocardial scar tissue with functioning tissue. Thus, there is a need for new therapeutics to regenerate damaged myocardium.

Recent developments in tissue engineering show promise for the creation of functional cardiac tissues without the need for biodegradable alternatives for the extracellular matrix (*1*). And we reported that cardiomyocyte sheets have been developed by using temperature-responsive culture dishes and these sheets survived in the back of nude rats and showed a spontaneous contraction over a long period of time (*2*). Recent reports suggested that cardiomyocyte sheets integrated with the impaired myocardium and improved cardiac performance in a rat model of ischemic myocardium (*3*).

This work was supported by a Grant-in-Aid for Scientific Research in Japan.

[1] Division of Cardiovascular Surgery, Department of Surgery, Faculty of Medicine, Osaka University Graduate School of Medicine, Suita, Osaka, Japan.

[2] Medical Center for Translational Research, Osaka University Hospital, Osaka, Japan.

[3] Department of Pathology, School of Allied Health Science, Faculty of Medicine, Osaka University Graduate School of Medicine, Suita, Osaka, Japan.

[4] Department of Investigative Radiology, National Cardiovascular Center Research Institute, Tokyo, Japan.

[5] Tokyo Women's Medical University Institute of Advanced Biomedical Engineering and Science, Tokyo, Japan.

[6] Address correspondence to: Yoshiki Sawa, M.D., Department of Cardiovascular Surgery, Osaka University Graduate School of Medicine, 2-2 Yamada-oka, Suita, Osaka 565-0871, Japan.
E-mail: sawa@surg1.med.osaka-u.ac.jp

S.M. participated in the writing of the paper; A.S. participated in research design; T.S. and Y.Y. participated in data analysis; T.Y., Y.I., N.K., and N.T. participated in the performance of research; N.M., H.I., T.S., T.O., and Y.S. participated in research design.

Received 15 December 2009. Revision requested 2 January 2010.
Accepted 6 May 2010.

ISSN 0041-1337/10/9004-364
DOI: 10.1097/TP.0b013e3181e6f201

And more recently, in the aim of clinical application, nonligature implantation of skeletal myoblast sheet regenerated the damaged myocardium and improved global cardiac function by attenuating the cardiac remodeling in the rat ligation model (*4*) and dilated cardiomyopathy hamster model (*5*). This cell delivery system by using cell sheets implantation showed better restoration of damaged myocardium compared with needle injection (*4*, *5*). Moreover, grafting of skeletal myoblast sheets attenuated cardiac remodeling and improved cardiac performance in pacing-induced canine heart failure model (*6*).

Given this body of evidence, we hypothesized that the autologous skeletal cell (SC) sheet implantation might remodel the chronic heart failure caused by ischemic injury.

Therefore, this preclinical study using Swine model was designed to test therapeutic effectiveness.

MATERIALS AND METHODS

Myocardial Infarction Model

"Principles of Laboratory Animal Care" formulated by the National Society for Medical Research and the "Guide for the Care and Use of Laboratory Animals" prepared by the Institute of Laboratory Animal Resource and published by the National Institutes of Health (NIH Publication No. 86-23, revised 1985). This animal experiment was approved by the Animal Care Committee of Osaka university graduate school of medicine. We induced acute myocardial infarction of 10 swine (20 kg, KEARI, Japan) by the following method. Swine were preanesthetized by intramuscular injection of ketamine hydrochloride 20 mg/kg (Ketalar, Sankyo, Japan) and xylazine 2 mg/kg (Seractar, Bayer). Animals were positioned spine and a 22-gauge indwelling needle (Surflo F&F, Terumo, Tokyo, Japan) was inserted in the central vein of the auricle. A three-way cock (Terufusion TS-TR2K, Terumo, Tokyo, Japan) was attached to the external cylinder of the indwelling needle, and an extension tube was connected for continuous anesthetic injection. The animals were intubated with an endotracheal cannula (6 Fr, Sheridan) using a pharyngoscope and then connected to an artificial respirator (Harvard, USA) by the cannula. Artificial respiration was implemented at a stroke volume of 200 to 300 mL/stroke and a stroke frequency of 20/min. The animals were continuously drip injected with propofol 6 mg/kg/hr (Diprivan, AstraZeneca) and vecuronium bromide 0.05 mg/kg/hr (Musculux, Sankyo Yell Yakuhin Co., Ltd., Japan) using a syringe pump (Terufusion TE-3310N, Terumo, Japan). The animal was then fixed in a recumbent position, so that the left thorax was exposed, and the outer layer of skin and muscles between the third and fourth ribs were dissected. After confirming the cutting into the thoracic cavity, the distance between the third and fourth ribs was widened with a rib spreader to allow a direct view of the left auricle and the LAD coronary artery. The pericardium was dissected along the LAD from the upper part of the left auricle (~6 cm) to expose the myocardium around the LAD. LAD on the proximal side below the left auricle from the myocardium was exfoliated for approximately 1 cm, and then a small amount of lidocaine hydrochloride jelly (Xylocaine jelly, AstraZeneca) was applied to allow for anesthetizing the area. An ameroid constrictor (COR-2.50-SS, Research Instruments) was then fit using No. 1 or 2 suture. The chest cavity was closed to end the procedures. The animals were randomly divided into two treatment groups: the first received autologous SC sheet implantation (SC group, n=5). For control, we have performed sham operation (C group, n=5).

Preparation of Skeletal Cell Sheets for Grafting

One week after implantation of ameroid constrictor on LAD, skeletal muscle weighing approximately 5 g was removed from the pretibial region with the porcine under general anesthesia. Following the addition of trypsin-ethylenediaminetetraacetic acid (Gibco, Grand Island, NY), excessive connective tissue was carefully removed to minimize the content of contaminating fibroblasts, and the muscle tissue was minced until the fine pieces formed a homogeneous mass. The specimens were then incubated at 37°C in shaker bath with 0.5% type 1 collagenase (Gibco) in Dulbecco's modified Eagle's medium (Gibco). After brief placement, the fluid was collected, and the same volume of culture medium, SkBM (Cambrex, Walkersville, MD) supplemented with fetal bovine serum (Thermo Trace, Melbourne, Australia), was added to halt the enzymatic digestion process. The cells were collected by centrifugation, and the putative SCs were seeded into 150 cm^2 polystyrene flasks after removal of fibroblasts by sedimentation for a few hours and cultured in SkBM at 37°C. During the culture process, we maintained cell densities at less than 70% confluence by carrying out passaging of cells for one time to prevent SCs from premature differentiation and fusion process resulting in myotubes formation. When the cells become approximately 70% confluent after 10 to 11 days cultivation, the cells were dissociated from the flasks with trypsin-ethylenediaminetetraacetic acid and reincubated on 100 mm temperature-responsive culture dishes (Cellseed, Tokyo, Japan) at 37°C with the cell numbers adjusted to 1×10^7 per dish. More than 90% of these cells were desmin positive (Fig. 1). After 4 days, the dishes were removed to refrigerator set at 20°C, and left there for approximately 30 min. During that time, the SC sheets detached spontaneously from the surfaces. Each sheet had a diameter of 30 to 40 mm and consisted of layers of SCs; the sheets were approximately 100-μm thick in cross-sectional views (Fig. 1). Approximately 10 sheets were obtained from the 5 g of skeletal muscle.

Implantation of Skeletal Cell Sheets

Autologous SC sheet implantation was performed in the swine 4 weeks after LAD ligation. Swine were anesthetized as mentioned above. The swine were exposed through the sternum. The infarct area was identified visually on the basis of surface scarring and abnormal wall motion. In the SC group, we implanted 10 SC sheets into the infarcted myocardium. The control group was treated similarly but received no SC sheets. Because pilling up four or more sheets caused the central necrosis of the myoblasts presumably because the lack of in oxygen supply, we decided to pile two or three layers of the SC sheet over the broad surface of the impaired heart.

Measurement of Cardiac Function

Swine were anesthetized as mentioned above. Cardiac ultrasonography was performed with a commercially available echocardiograph, SONOS 5500 (PHILIPS Electronics, Tokyo, Japan). A 3-MHz annular array transducer was placed on a layer of acoustic coupling gel that was applied to the left hemithorax. Swine were examined in a shallow left lateral decubitus position. The heart was first imaged in the two-dimensional mode in short-axis views at the level of the largest left ventricle (LV) diameter. The calculation of the LV volume was based on the LV short-axis area using AQ system (*7*). And fractional area shortening (FAS) of the LV diastolic was calculated as follows:

$$\text{FAS}\,(\%)=[(\text{LVend-diastolic area}-\text{LV end-systolic area [ESA]})/\text{LV end-diastolic area}]\times 100$$

These data are presented as the average of measurements of two or three selected beats.

Quantification of Regional Diastolic and Systolic Function by Color Kinesis

Diastolic CK images were obtained using a commercially available ultrasound system (SONOS 5500, Philips Medical Systems) from the LV midpapillary short-axis view for the determination of wall motion asynchrony as previously reported (*8*). CK examined every image pixel within the region of interest, which was drawn around the LV cavity, classifying it as blood or tissue based on integrated backscatter data. During diastole, each pixel was tracked into the next frame, and pixel transitions from endocardium to blood were detected and interpreted as diastolic endocardial motions. These pixel transitions were encoded using a color hue specific to each consecutive video frame, so that each color represents the excursion of that segment during a 33-ms period of time. The sites of regional LV diastolic wall motion or regions of interest were set on the basis of standard segmentation models: anterior, lateral, posterior, inferior, anteroseptal wall. The CK diastolic index was defined as the LV segmental filling fraction

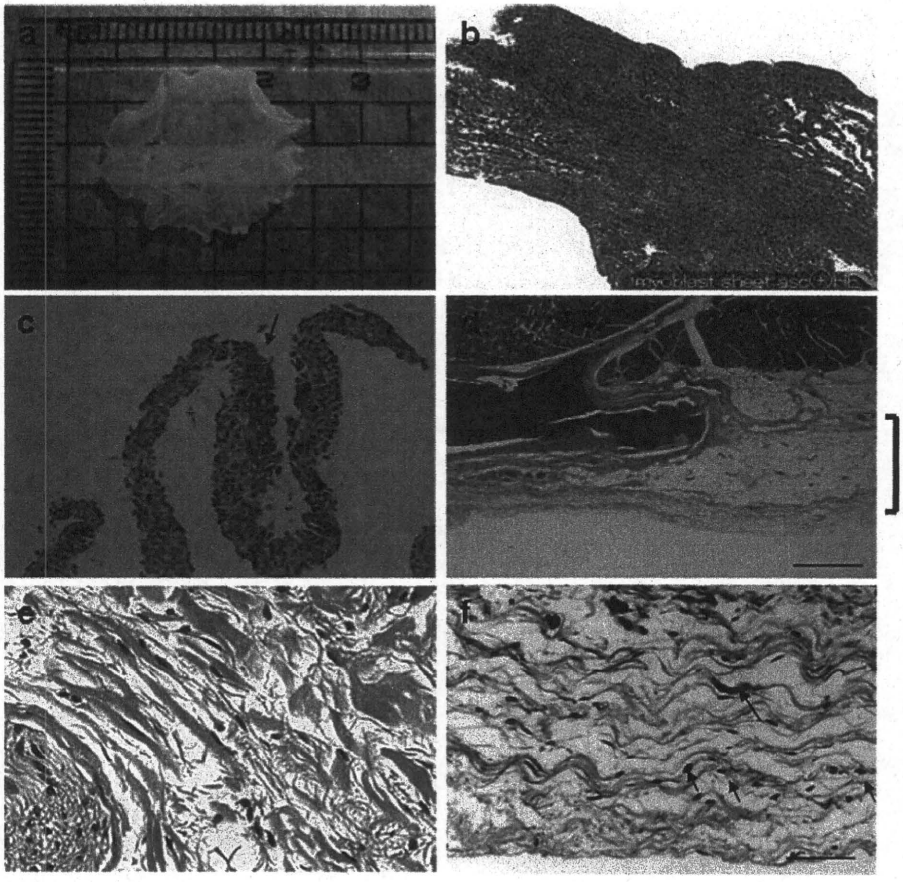

FIGURE 1. Histological characteristics of skeletal cell (SC) sheet. (a) SC sheet detached from the Poly (*N*-isopropylacrylamide)-grafted polystyrene by lowering the temperature. Its size is approximately 3 cm×2 cm^2. (b) Hematoxylin-eosin (H&E) stain; cross-sectional views of SC sheet in vitro. SC sheet demonstrates homogeneous heart-like tissue. (c) Not so many smooth muscle cells were detected in the SC sheets. The *arrow* indicates the smooth muscle cells in the SC sheet. (d) H&E stain revealed that SC sheets attached on the surface of epicardium. *Left square bracket* indicates implanted SC sheets. (e) Oval-shaped cells that showed positive for eosin in cytoplasm were detected in the SC group microscopically in some layers over epicardium. (f) Elastica Masson Goldner showed that oval-shaped cells that supposed to origin from skeletal tissue exist in the transplantation site. *Arrows* indicate oval-shaped cells that suppose to be originated form skeletal tissue.

during the first 30% of the diastolic filling time (LV segmental cavity area expansion during the first 30% of diastole, divided by the segmental end-diastolic LV cavity area expansion, expressed as a percentage). We introduced the use of color kinesis method that displays endocardial motion in real time to evaluate the regional systolic function (*8*).

Histopathology

LV myocardium specimens were obtained 6 months after the SC sheet implantation. Each specimen was fixed with 10% buffered formalin and embedded in paraffin. A few serial sections were prepared from each specimen and stained with hematoxylin-eosin (H&E) stain and elastica Masson-Goldner for histological examination or with Masson's trichrome stain to assess the collagen content.

To label vascular endothelial cells so that the blood vessels could be counted, immunohistochemical staining of factor VIII-related antigen was performed according to a modified protocol. Frozen sections were fixed with a 2% paraformaldehyde solution in phosphate-buffered saline (PBS) for 5 min at room temperature, immersed in methanol with 3% hydrogen peroxide for 15 min, then washed with PBS. The samples were covered with bovine serum albumin solution (DAKO LSAB Kit DAKO CORPORATION, Denmark) for 10 min to block nonspecific reactions. The specimens were incubated overnight with an Enhanced Polymer One-Step Staining (EPOS)-conjugated antibody against factor VIII-related antigen coupled with horseradish peroxidase (DAKO EPOS Anti-Human Von Wille brand Factor/HRP, DAKO, Denmark). After the samples were washed with PBS, they were immersed in diaminobenzidine solution (0.3 mg/mL diaminobenzidine in PBS) to obtain positive staining. Ten different fields at 200× magnification were randomly selected, and the number of the stained vascular endothelial cells in each field was counted under a light microscope. The result was expressed as the number of blood vessels per square millimeter.

The following antibodies against smooth muscle cells and skeletal myosin (slow) were used to evaluate the existence of SCs: primary antibodies, anti-smooth muscle actin (clone 1A4, DAKO) antiskeletal myosin (slow) (clone NOQ7.5.4D, Sigma); secondary antibodies, anti-mouse Ig biotinylate (DAKO).

Picro-sirius red staining for the assessment of myocardial fibrosis or periodic acid-Schiff staining for that of cardiomyocyte hypertrophy was performed as described (*9*).

Positron Emission Tomography Procedure

We performed positron emission tomography (PET) studies on pigs which were transplanted SC sheets and control by using ^{15}0-water and ^{18}F-FDG. The pigs were anesthetized by the introduction of pentobarbital followed by continuous inhalation of propofol (4 mg/kg/hr) and were placed supine on the bed of the scanner. PET was performed using a HEADTOME-III tomograph (Shimadzu, Kyoto, Japan) and data were analyzed as described elsewhere (*10*).

Holter Electrocardiography

To evaluate arrhythmia we used Holter electrocardiography (ECG) for 24 hours. We checked arrhythmia by checking the number of ventricular premature beat after SC sheet implantation in myocardial infarction porcine (n=3).

Data Analysis

Data are expressed as means ± SEM and subjected to multiple analysis of variance (ANOVA) using the StatView 5.0 program (Abacus Concepts, Berkeley, CA). Echocardiographic data were first analyzed by two-way repeated measurement ANOVA for differences across the whole time course, and one-way ANOVA with the Tukey-Kramer posthoc test was used to verify the significant for the specific comparison at each time point. To assess the significance of the differences between individual groups concerning other numeral data, statistical evaluation was performed with an unpaired *t* test. Statistical significance was determined as having a *P* value less than 0.05.

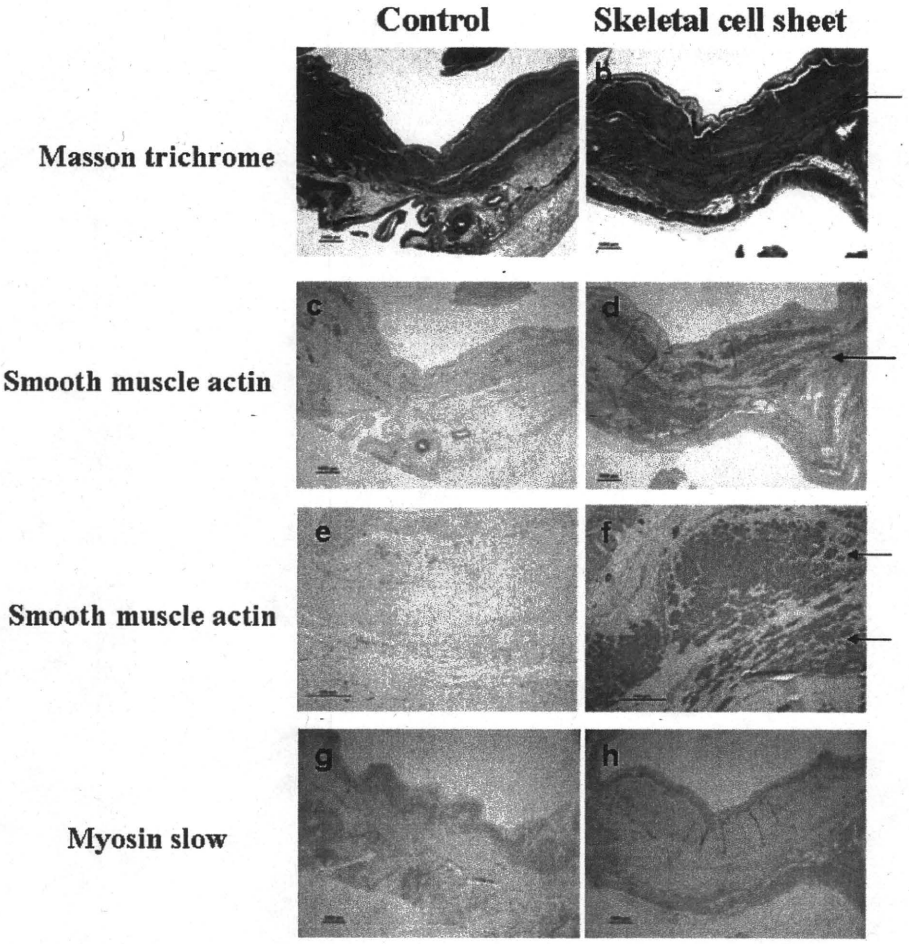

FIGURE 2. The detection of a large quantity of skeletal cells (SCs) in the center of the scar. (a and b) Masson trichrome staining reveals that some layered muscles are detected in the center of the scar in the SC sheet transplantation group, whereas not in the control. (c–f) Smooth muscle actin staining demonstrated that well-developed smooth muscle cells occupied in the center of the scar in the SC sheet transplantation group, whereas only smooth muscle cells which are formed vasculature are detected in the control. (g and h) Slow-type myosin staining showed that no positive cells exist in the center of the scar. This means that SCs which are detected in the center of the scar are not the residual myocyte after infarction.

RESULTS

Characteristics of Myoblast Sheet

We obtained monolayered myoblast sheets by lowering the temperature, which released them from the Poly(*N*-isopropylacrylamide)-grafted polystyrene. Its size is approximately 3 cm×2 cm^2 (Fig. 1a). H&E staining demonstrated that SC sheet contained a lot of SCs and SC sheets had an appearance of homogenous tissue, which thickness of one SC sheet was approximately 100 μm (Fig. 1b). Some smooth muscle cells are detected in the SC sheets, but those cells are not majority (Fig. 1c).

Histological Assessment

H&E staining demonstrated that transplanted SC sheets were attached in the epicardium (Fig. 1d) and oval-shaped cell that showed positive for eosin in cytoplasm were detected in the SC group microscopically in some layers over epicardium (Fig. 1e). Elastica Masson-Goldner showed that oval-shaped cells that supposed to origin from skeletal tissue exist in the transplantation site (Fig. 1f). These cells were not seen in the control group. And the SC group demonstrated decrease in the cross-sectional LV area compared with the C groups (Fig. 2a). Masson's trichrome staining showed that clustered SCs were detected in the center of the scar, whereas clustered SCs were not detected in the C group (Fig. 2a, b). Many clusters of well-developed smooth muscle cells exist in the center of the whole scar in the SC group, whereas in the C group, smooth muscle cells which formed vasculature exist in the scar (Fig. 2c–f). Although slow-type myosin-positive cells exist only on the endocardium and epicardium, those cells were not detected in the center of scar (Fig. 2g,h). So these figures depict that the skeletal muscle cells that exist in the center of the scar is not residual myocyte after infarction.

Quantification of Histopathology

In the SC group, vascular density was found to be significantly higher than in the C groups (SC vs. C=217.1±30.2 vs. 114.2±18.2 /field; $P<0.05$) (Fig. 3b).

Picro-sirius red staining demonstrated that % fibrosis was significantly reduced in the SC group compared with the C group (SC vs. C=1.6±0.2 vs. 3.1±0.3%; $P<0.05$) (Fig. 3b). Periodic acid-Schiff staining showed that cell diameter was significantly shorter in the SC group than the C group (SC vs. C=10.7±0.3 vs. 18.3±1.4 μm; $P<0.05$) (Fig. 3b).

These histological findings were universally identified in the native myocardial tissue without distinction of distance from the grafted region.

Functional Assessment of the Infarcted Myocardium

The FAS and LV end-ESA scores at baseline were not significantly different between the two groups.

Three months after the implantation, two-dimensional echocardiography showed significant improvement of the

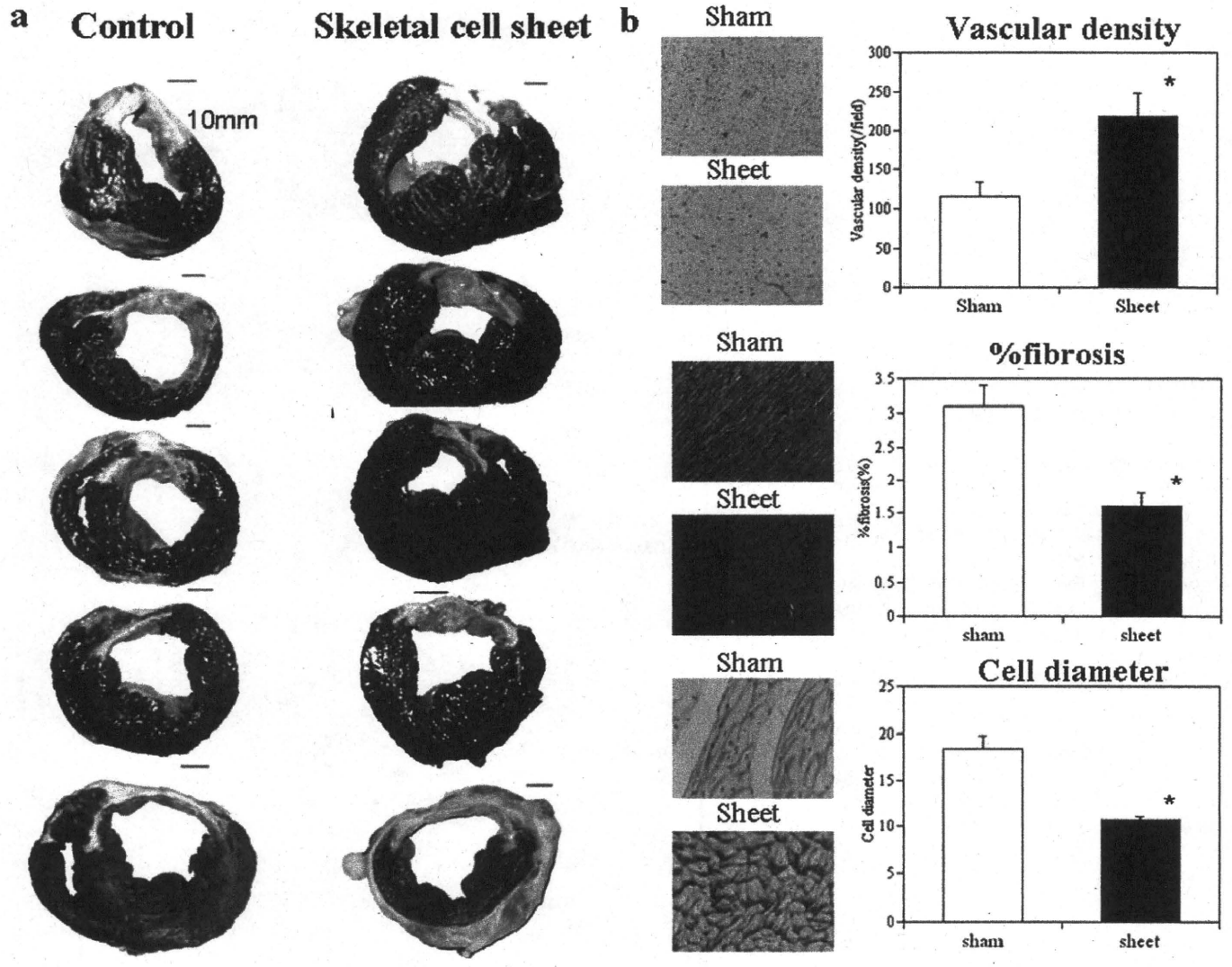

FIGURE 3. Macroscopic images of impaired myocardium receiving skeletal cell (SC) sheets and histological evaluation. (a) In the SC group, the anterior wall has recovered compared with the C group. In the SC group, the short axis area of the left ventricle (LV) is small compared with the C groups. In contrast, the C group shows a dilated LV and the anterior wall is thinner than in the SC groups. (b) Histological evaluation. Vascular density: the SC group showed a significant improvement in vascular density as assessed by immunostaining for the factor VIII-related antigen. *P less than 0.05 vs. C. The ratio of fibrosis-occupied area (% fibrosis) at a site remote from the infarcted heart region: picro-sirius red staining demonstrated that % fibrosis at a site remote from the infarcted heart region was significantly reduced in the SC group compared with the C group. *P less than 0.05 vs. C. The diameter of cardiomyocyte: the diameter of cardiomyocyte is significantly shorter in the SC group than the C group. *P less than 0.05 vs. C.

FIGURE 4. Global functional effects of infarcted myocardium receiving the implant. Global systolic function assessed by the fractional area shortening (FAS) (a) was significantly improved in the skeletal cell (SC) group 3 months after transplantation, and these functional improvements were preserved 6 months after SC sheet implantation. (b) The end-systolic area (ESA) was significantly smaller in the SC group than in the C groups 3 and 6 months after implantation. *P less than 0.05 vs. C, ■: SC sheet, ●: control.

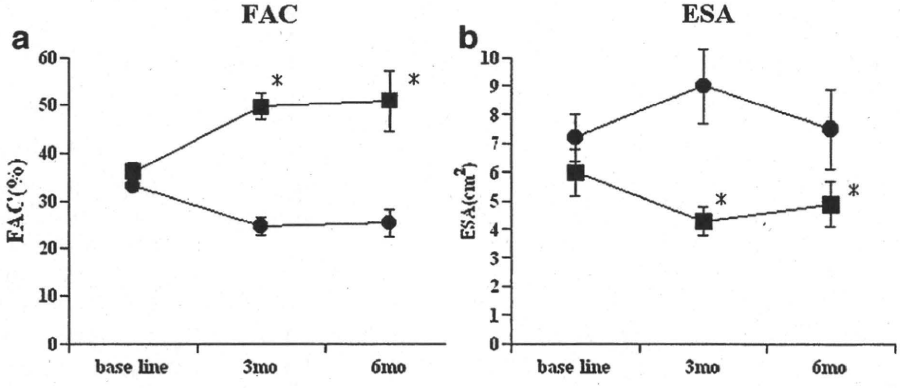

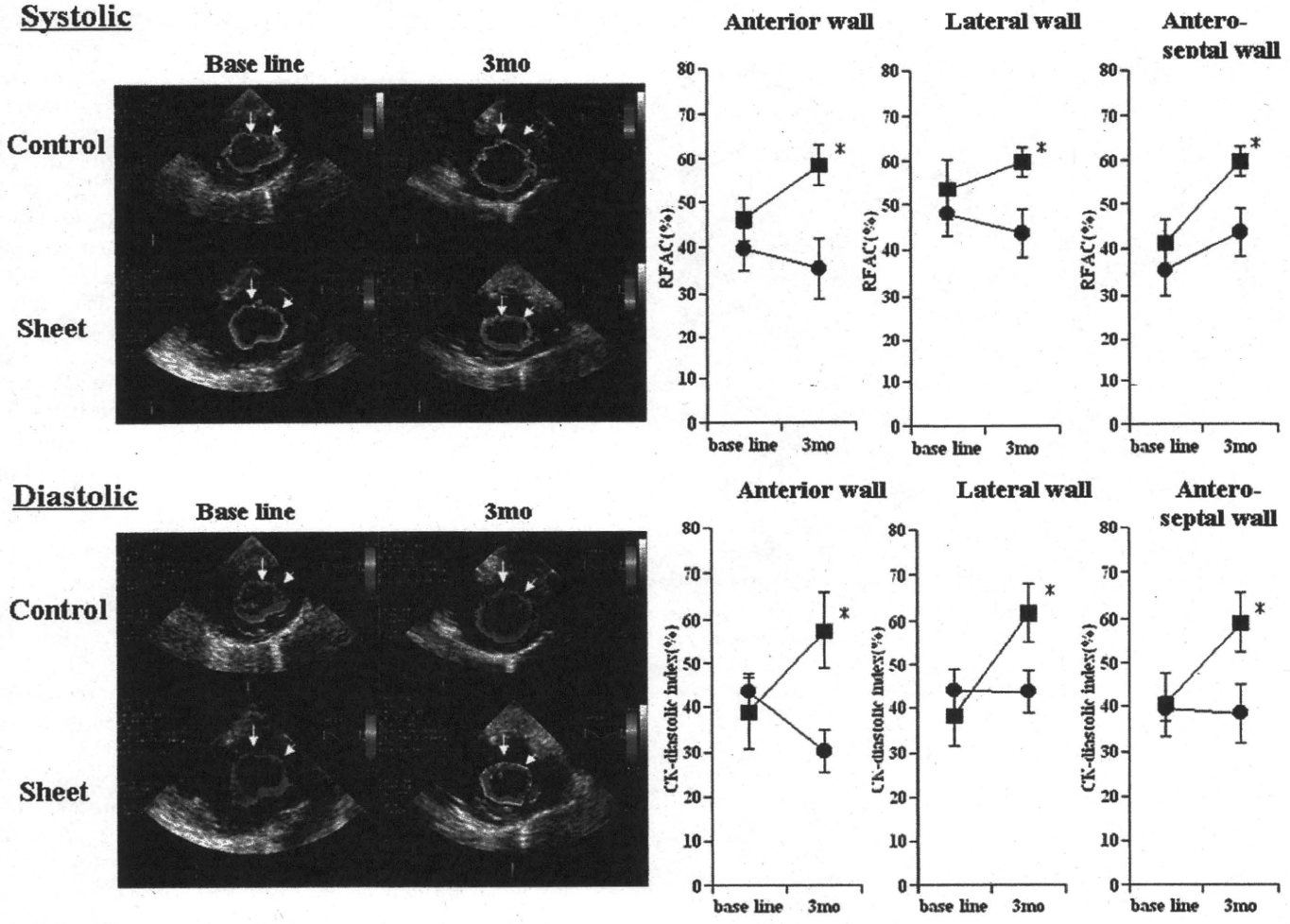

FIGURE 5. Systolic function: regional systolic function was significantly recovered in the skeletal cell (SC) group 3 months after implantation compared with the C group in the anterior, lateral, and anteroseptal wall. *P less than 0.05. Diastolic function: regional dysfunction was significantly recovered in the SC group 3 months after implantation compared with the C group in the anterior, lateral, and anteroseptal wall. Before treatment, diastolic dysfunction was observed in the infarction area of myocardium and the regional delayed relaxation was detected in the remote site of infarction by color kinesis. But this phenomenon was disappeared after SC sheet implantation. *P less than 0.05, ■: SC sheet, ●: control.

FAS (Fig. 4a) in the SC group compared with the C group (SC vs. C=49.5±2.8 vs. 24.6±2.0%, $P<0.05$). These functional improvements were preserved 6 months after implantation (SC vs. C=50.8±6.4 vs. 25.3±2.8%, $P<0.05$). The ESA was significantly smaller in the SC group than in the C group 3 months after the implantation (SC vs. C=4.3±0.5 vs. 9±1.3 cm^2, $P<0.05$) (Fig. 4b). These attenuation of LV dilatation were preserved 6 months after implantation (SC vs. C=4.9±0.8 vs. 7.5±1.4 cm^2, $P<0.05$). During this long-term observation, all SC sheet-treated animals were alive and exhibited no malignant arrhythmia assessed by 24-hour Holter ECG once a week (data not shown).

Before treatment, diastolic dysfunction was observed in the infarction area of myocardium and the regional delayed relaxation was detected in the remote site of infarction by color kinesis. After 3 months after implantation, CK-diastolic index in the lateral (SC vs. C=61.7±6.4 vs. 43.7±4.8%, $P<0.05$), anterior (SC vs. C=57.4±8.6 vs. 30.2±4.7%, $P<0.05$), and anteroseptal (SC vs. C=59±6.6 vs. 38.4±6.6%, $P<0.05$) segment were significantly ameliorated in the SC group compared with the C group, and regional systolic function in transplanted site was significantly improved in the SC group while not in the C groups (SC vs. C: lateral, 59.8±3.3 vs. 43.6±5.4%, $P<0.05$; anterior, 58.5±4.5 vs. 35.4±6.6%, $P<0.05$; anteroseptal, 59.8±3.3 vs. 43.6±5.4%, $P<0.05$), respectively (Fig. 5).

We could detect no ventricular premature beat for 24 hr by the Holter ECG in three myocardial infarction porcine received SC sheets.

Regional Myocardial Blood Flow and Residual Myocardial Tissue

PET study by using ^{15}0-water showed that the myocardial water-perfusable tissue fraction and myocardial blood flow were higher in the anterior wall where SC sheets were implanted compared with the myocardium receiving no sheets. These data depict that myocardial blood flow was better and microcirculation in the infarcted myocardium was preserved in the SC sheets implanted myocardium. PET study by using ^{18}F-FDG revealed that more viable myocardial tis-

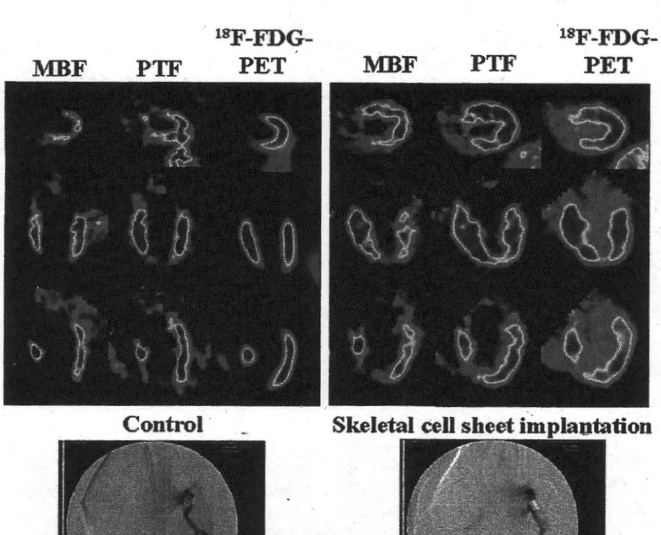

FIGURE 6. Positron emission tomography (PET) study revealed that perfusable tissue fraction (PTF) and myocardial blood flow (MBF) were higher and more viable myocardial tissues were preserved in the skeletal cell sheets implanted site compared with the myocardium receiving no sheets.

sues were preserved in the skeletal sheet implanted myocardium compared with the myocardium receiving no sheets. Coronary angiography revealed that LAD was occluded by the ameroid constrictor in both cases (Fig. 6).

DISCUSSION

Over the past several years, increasing awareness of the shortcomings of heart transplantation and left ventricular assist system implantation has led cardiovascular surgeons to consider alternative means of treating end-stage heart failure. In clinical setting, cellular cardiomyoplasty has been reported to have the potential of fundamental regenerative capability and has already been introduced in clinical trials with skeletal myoblast (*11*) or bone marrow mononuclear cells (*12*), and results suggest that it is a relatively feasible and safety therapy as a therapeutic angiogenesis. In this setting, cardiac tissue implantation was proposed to the treatment of end-staged heart failure as a new concept of regenerative therapy and experimentally some groups depicted it's effectiveness in the damaged myocardium (*13*, *14*). We also reported that cell sheets have great impacts on restoration of damaged myocardium in the rat infarction model (*3*, *4*) and dilated cardiomyopathy hamster (*5*). To convince the effectiveness of cell sheets in preclinical trial, we examined whether autologous SC sheets implantation might become one of the armamentarium of regenerative therapy for chronic heart failure caused by myocardial infarction in the porcine model.

The potential added advantages of the cell sheet implantation method include the implantation of a high number of cells with minimum cell loss. In contrast, the injection method is associated with a high loss of cells or surface proteins due to the trypsin treatment. Despite a high number of cell loss in needle injection, the cell sheet implantation method might provide the advantages of a higher number of cell implantation without cellular community destruction, leading the more improvement of cardiac performance rather than cell injection method (*4*). In case of needle injection, inflammation accompanied with destruction of myocardium induced by needle injection promotes graft death after cell transplantation (*15*).

To examine the effects of the SC sheet implantation therapy, we analyzed cardiac function and performed a histological assessment of the infarcted heart after SC sheet transplantation in a swine infarction model. SC sheet implantation therapy significantly induced angiogenesis, reduction of fibrosis histologically. And cell diameter of host myocyte was significantly attenuated its hypertrophy compared with the no treatment group. PET study revealed the better regional blood perfusion and better regional myocardial viability in the myocardium receiving cell sheets compared with the myocardium receiving no sheets.

Moreover, SC sheet implantation induced functional recovery of damaged myocardium. Especially, we demonstrated that the regional diastolic and systolic dysfunction was well recovered in the sheet implanted group. Before treatment, diastolic dysfunction of infarcted area and regional delayed relaxation of noninfarcted site were detected by color kinesis in the porcine infracted myocardium. After treatment, diastolic dysfunction of infarcted site was significantly recovered and the phenomenon of regional delayed relaxation in noninfarcted site was not seen. Presumably, implanted elastic myoblast sheets and a large quantity of well-developed smooth muscle cells, which are detected in the center of the scar, improved the regional diastolic dysfunction of implanted site. Although SC sheet can not contract in vivo after implantation, this recovery of diastolic disassociation of LV might result in the recovery of systolic dysfunction.

To the best of our knowledge, this is the first report in which tissue-engineered SC sheets implantation was successfully used to improve cardiac performance in a large animal model of ischemic myocardium according to the Laplace's theory.

The mechanisms of the restoration of damaged myocardium by SC sheet implantation might be complicated and many pathways might affect the recovery of ischemic myocardium. Recent reports depict that cell sheets enhance the recruitment of hematopoietic stem cells through the release of stromal-derived factor 1 (*4*). The fact of thicker anterior wall and the improvement of regional function might depend on both the recruitment of cytokine releasing stem cells, survival of grafted cells, and well-developed smooth muscle cells. And these cells might have good elasticity and these elastic cells and tissues softened the stiffness of anterior wall in association with the attenuating fibrosis even in the infarct area. This reduced stiffness of anterior wall might lead to the improvement of the diastolic dysfunction. Transplanted SCs cannot differentiate into cardiomyocyte anymore, but regional systolic function improved in the transplanted site. Probably, the improvement of regional diastolic function due to elastic cells might be responsible for the restoration of regional systolic dysfunction. Recent reports demonstrated that regional left ventricular myocardial relaxation was closely related to regional myocardial contraction (*16*) and the improvement of regional myocardial relaxation leads to the

recovery of global diastolic function (*17*). Moreover, the improvement of regional systolic function is closely related to global systolic function (*18*). We assume that this theory about the relationship between diastolic and systolic function is one of the mechanisms about the improvement of diastolic and systolic function in the cell sheet transplanted myocardium.

Question is why the well-developed smooth muscle cells exist in the center of the scar in the SC sheet group after transplantation despite a small quantity of smooth muscle cells in the SC sheet? Does a small quantity of smooth muscle cells in the SC sheet proliferate after transplantation? Do progenitor cells in the SC sheet differentiate to smooth muscle cells? Do progenitor cells or smooth muscle cells in the host myocardium migrate to the implanted site and proliferate? To the regret, there is no data to answer these questions exactly in this article and more detailed studies are needed to elucidate this important question.

Some reports depicted that the expression of hepatocyte growth factor (HGF) in the myoblast sheet transplanted ischemic myocardium is higher compared with the nontransplanted ischemic myocardium (*4*). HGF has an antifibrotic activity both through the activation of a matrix degradation pathway (*19*), restoration of cytoskeletal proteins on cardiomyocyte (*20*), and induce angiogenesis in the ischemic myocardium (*21*). Our study demonstrated that % fibrosis was significantly reduced in the SC sheet transplanted group. This paracrine secretion of HGF from SC sheets might attribute the reduction of % fibrosis. In our study, much more factor VIII-positive cells are detected in the SC sheet transplanted myocardium. This might be induced by paracrine secretion of HGF and angiogenesis might rescue the ischemic host cardiomyocyte and bring about the improvement of the distressed function of host cardiomyocyte. The distressed cytoskeletal proteins on the cardiomyocyte in the ischemic myocardium might be reorganized by the HGF secreted from skeletal sheet and the restoration of cytoskeletal proteins might lead to the improvement of cardiac function. And some reports demonstrated that myoblast sheets maintain the distressed cytoskeletal proteins on the host cardiomyocyte in the dilated cardiomyopathy hamster model (*5*). Consequently, cell sheet treatment is appropriate for recovery of ischemic cardiomyopathy. Recent research works demonstrated that several regenerative factors such as insulin-like growth factor-1 (*22*) and Thymosin b4 (*23*) were expressed in the rat ischemic myocardium model after myoblast sheet implantation by reverse-transcriptase polymerase chain reaction analysis (data not shown). After myoblast sheet transplantation to ischemic myocardium, several regenerative factors are expressed in the transplanted site, and these long-term and low-dosed expressed regenerative factors might cooperatively restore the damaged myocardium.

We could find no ventricular premature beat analyzed by Holter ECG after SC sheet implantation. We have already proved that in the rat infarction model, arrhythmia is less in the SC sheet implantation group compared with the needle injection group and this work represented that more monocyte chemotactic protein-1-positive cells and CD11b (macrophage marker)-positive cells were detected in the needle injection group compared with SC sheet implantation (data not shown). We speculate that needles destroy the myocardium and this destroyed myocardium may induce the inflammation and this inflammation may induce the arrhythmia. Conversely, SC sheet implantation technique normally doses not destroy the myocardium when they are implanted to recipient heart. Moreover, SC sheet will survive on the epicardium and electrical wave originated from implanted myoblasts may not deliver to the recipient myocardium directly. But when we implant myoblasts by needle injection, implanted myoblasts survive in the center of the myocardium and electrical wave will deliver to the myocardium directly, leading to the arrhythmia.

In conclusion, we have preclinically demonstrated SC sheets produced histologically and functionally apparent prevented the deterioration of the impaired myocardium in the swine model. These data provide a basis for attempting clinical cell sheet implantation in ischemic disease as the armamentarium to promote the regeneration of chronic heart failure caused by myocardial infarction.

ACKNOWLEDGMENTS

The authors thank Shigeru Matsumi and Masako Yokoyama for their excellent technical assistance.

REFERENCES

1. Shimizu T, Yamato M, Akutsu T, et al. Fabrication of pulsatile cardiac tissue grafts using a novel 3-dimensional cell sheet manipulation technique and temperature-responsive cell culture surfaces. *Circ Res* 2002; 90: e40.
2. Shimizu T, Sekine H, Isoi Y, et al. Long-term survival and growth of pulsatile myocardial tissue grafts engineered by the layering of cardiomyocyte sheets. *Tissue Eng* 2006; 12: 499.
3. Miyagawa S, Sawa Y, Sakakida S, et al. Tissue cardiomyoplasty using bioengineered contractile cardiomyocyte sheets to repair damaged myocardium: Their integration with recipient myocardium. *Transplantation* 2005; 80: 1586.
4. Memon IA, Sawa Y, Fukushima N, et al. Repair of impaired myocardium by means of implantation of engineered autologous myoblast sheets. *J Thorac Cardiovasc Surg* 2005; 130: 1333.
5. Kondoh H, Sawa Y, Miyagawa S, et al. Longer preservation of cardiac performance by sheet-shaped myoblast implantation in dilated cardiomyopathic hamsters. *Cardiovasc Res* 2006; 69: 466.
6. Hata H, Matsumiya G, Miyagawa S, et al. Grafted skeletal myoblast sheets attenuate myocardial remodeling in pacing-induced canine heart failure model. *J Thorac Cardiovasc Surg* 2006; 132: 918.
7. Mor-Avi V, Vignon P, Bales AC, et al. Acoustic quantification indexes of left ventricular size and function: Effects of signal averaging. *J Am Soc Echocardiogr* 1998; 11: 792.
8. Ishii K, Miwa K, Makita T, et al. Prolonged postischemic regional left ventricular delayed relaxation or diastolic asynchrony detected by color kinesis following coronary vasospasm. *Am J Cardiol* 2003; 91: 1366.
9. Fukui S, Kitagawa-Sakakida S, Kawamata S, et al. Therapeutic effect of midkine on cardiac remodeling in infarcted rat hearts. *Ann Thorac Surg* 2008; 85: 562.
10. Iida H, Yokoyama I, Agostini D, et al. Quantitative assessment of regional myocardial blood flow using oxygen-15-labelled water and positron emission tomography: A multicentre evaluation in Japan. *Eur J Nucl Med* 2000; 27: 192.
11. Dib N, Michler RE, Pagani FD, et al. Safety and feasibility of autologous myoblast transplantation in patients with ischemic cardiomyopathy: Four-year follow-up. *Circulation* 2005; 112: 1748.
12. Perin EC, Dohmann HF, Borojevic R, et al. Transendocardial, autologous bone marrow cell transplantation for severe, chronic ischemic heart failure. *Circulation* 2003; 107: 2294.
13. Leor J, Aboulafia-Etzion S, Dar A, et al. Bioengineered cardiac grafts. A new approach to repair the infarcted myocardium? *Circulation* 2000; 102(suppl III): III-56.

14. Li RK, Jia ZQ, Weisel RD, et al. Survival and function of bioengineered cardiac grafts. *Circulation* 1999; 100(suppl II): II-63.
15. Suzuki K, Murtuza B, Beauchamp JR, et al. Role of interleukin-1beta in acute inflammation and graft death after cell transplantation to the heart. *Circulation* 2004; 110(11 suppl 1): II-219.
16. Tanaka H, Kawai H, Tatsumi K, et al. Relationship between regional and global left ventricular systolic and diastolic function in patients with coronary artery disease assessed by strain rate imaging. *Circ J* 2007; 71: 517.
17. Tanaka H, Kawai H, Tatsumi K, et al. Improved regional myocardial diastolic function assessed by strain rate imaging in patients with coronary artery disease undergoing percutaneous coronary intervention. *J Am Soc Echocardiogr* 2006; 19: 756.
18. Moller JE, Hillis GS, Oh JK, et al. Wall motion score index and ejection fraction for risk stratification after acute myocardial infarction. *Am Heart J* 2006; 151: 419.
19. Liu Y, Rajur K, Tolbert E, et al. Endogenous hepatocyte growth factor ameliorates chronic renal injury by activating matrix degradation pathways. *Kidney Int* 2000; 58: 2028.
20. Miyagawa S, Sawa Y, Taketani S, et al. Myocardial regeneration therapy for heart failure: Hepatocyte growth factor enhances the effect of cellular cardiomyoplasty. *Circulation* 2002; 105: 2556.
21. Taniyama Y, Morishita R, Aoki M, et al. Therapeutic angiogenesis induced by human hepatocyte growth factor gene in rat and rabbit hindlimb ischemia models: Preclinical study for treatment of peripheral arterial disease. *Gene Ther* 2001; 8: 181.
22. Li Q, Li B, Wang X, et al. Overexpression of insulin-like growth factor-1 in mice protects from myocyte death after infarction, attenuating ventricular dilation, wall stress, and cardiac hypertrophy. *J Clin Invest* 1997; 100: 1991.
23. Bock-Marquette I, Saxena A, White MD, et al. Thymosin beta4 activates integrin-linked kinase and promotes cardiac cell migration, survival and cardiac repair. *Nature* 2004; 432: 466.

TISSUE ENGINEERING: Part A
Volume 16, Number 4, 2010

DOI: 10.1089/ten.tea.2009.0386

Reduction of *N*-Glycolylneuraminic Acid Xenoantigen on Human Adipose Tissue-Derived Stromal Cells/ Mesenchymal Stem Cells Leads to Safer and More Useful Cell Sources for Various Stem Cell Therapies

Hiroshi Komoda, M.D., Ph.D.,[1,2,*] Hanayuki Okura, M.S.,[1,3,4,*] Chun Man Lee, M.D., Ph.D.,[1,5] Nagako Sougawa, D.M.D., Ph.D.,[1] Tomoaki Iwayama, D.M.D.,[6] Tomoko Hashikawa, D.M.D., Ph.D.,[6] Ayami Saga, M.S.,[1] Aya Yamamoto-Kakuta, B.S.,[1] Akihiro Ichinose, M.D., Ph.D.,[7] Shinya Murakami, D.M.D., Ph.D.,[6] Yoshiki Sawa, M.D., Ph.D.,[3,5] and Akifumi Matsuyama, M.D., Ph.D.[1]

Adipose tissue is an attractive source for somatic stem cell therapy. Currently, human adipose tissue-derived stromal cells/mesenchymal stem cells (hADSCs/MSCs) are cultured with fetal bovine serum (FBS). Recently, however, not only human embryonic stem cell lines cultured on mouse feeder cells but also bone marrow-derived human MSCs cultured with FBS were reported to express *N*-glycolylneuraminic acid (Neu5Gc) xenoantigen. Human serum contains high titers of natural preformed antibodies against Neu5Gc. We studied the presence of Neu5Gc on hADSCs/MSCs cultured with FBS and human immune response mediated by Neu5Gc. Our data indicated that hADSCs/MSCs cultured with FBS expressed Neu5Gc and that human natural preformed antibodies could bind to hADSCs/MSCs. However, hADSCs/MSCs express complement regulatory proteins such as CD46, CD55, and CD59 and are largely resistant to complement-mediated cytotoxicity. hADSCs/MSCs cultured with FBS could be injured by antibody-dependent cell-mediated cytotoxicity mechanism. Further, human monocyte-derived macrophages could phagocytose hADSCs/MSCs cultured with FBS and this phagocytic activity was increased in the presence of human serum. Culturing hADSCs/MSCs with heat-inactivated human serum for a week could markedly reduce Neu5Gc on hADSCs/MSCs and prevent immune responses mediated by Neu5Gc, such as binding of human natural preformed antibodies, antibody-dependent cell-mediated cytotoxicity, and phagocytosis. Adipogenic and osteogenic differentiation potentials of hADSCs/MSCs cultured with heat-inactivated human serum were not less than that of those cultured with FBS. For stem cell therapies based on hADSCs/MSCs, hADSCs/MSCs that presented Neu5Gc on their cell surfaces after exposure to FBS should be cleaned up to be rescued from xenogeneic rejection.

Introduction

Adipose tissue is an attractive source for somatic cell therapy, because it is safe and abundant and many investigators have reported that the stromal cells derived from adipose tissue (adipose tissue-derived stromal cells [ADSCs]) could differentiate into various cell types.[1–4] ADSCs are also referred to as adipose tissue-derived mesenchymal stem cells (MSCs). Human ADSCs (hADSCs)/MSCs are very similar to bone marrow (BM)-derived human MSCs (hMSCs) and therefore reveal differentiation potential similar to BM-derived hMSCs.[5–7]

For stem cell therapies based on hMSCs including hADSCs/MSCs, it is essential that stem cells are handled and cultured in a manner that guarantees the efficacy and safety of the cellular therapy product. One such aspect is the choice

[1]Department of Somatic Stem Cell Therapy, Foundation for Biomedical Research and Innovation, Kobe, Hyogo, Japan.
[2]Department of Internal Medicine, National Hospital Organization Chiba Medical Center, Chiba, Japan.
[3]Department of Surgery, Osaka University Graduate School of Medicine, Suita, Osaka, Japan.
[4]Japan Society for the Promotion of Science, Tokyo, Japan.
[5]Medical Center for Translational Research, Osaka University Hospital, Suita, Osaka, Japan.
[6]Department of Periodontology, Division of Oral Biology and Disease Control, Osaka University Graduate School of Dentistry, Osaka, Japan.
[7]Department of Plastic Surgery, Kobe University Hospital, Kobe, Hyogo, Japan.
*These authors contributed equally to this work.

of cell culture medium and supplements. In principle, most investigators agree that all animal materials should be avoided to maximize product safety. Currently, however, hADSCs/MSCs are cultured with fetal bovine serum (FBS), and the clinical efficacy of BM-derived hMSCs in human disease has been investigated using hMSCs cultured with FBS in a number of clinical trials.[8–12]

Recently, not only human embryonic stem cell (hESC) lines cultured on mouse feeder cells but also BM-derived hMSCs cultured with FBS were reported to express *N*-glycolylneuraminic acid (Neu5Gc) xenoantigen,[13,14] the so-called Hanganutziu–Deicher antigen.[15] Humans are incapable of synthesizing the common mammalian sialic acid, Neu5Gc, because of an *Alu* transposon-mediated inactivation of the cytidine monophosphate (CMP)-*N*-acetylneuraminic acid hydroxylase gene.[16,17] Despite this, both hESC lines and BM-derived hMSCs were reported to express the Neu5Gc, apparently originating from the mouse feeder layers, animal-derived components, and FBS.[13,14] The significant levels of Neu5Gc found on the surface of hESCs and hMSCs evidently originate from a Trojan Horse pathway involving endocytosis of extracellular glycoconjugates, delivery to the lysosome, release of Neu5Gc by lysosomal sialidase, active transport to the cytoplasm through the lysosomal sialic acid transporter, activation by CMP, and addition to nascent glycoproteins and glycolipids in the secretory pathway.[18] It is also possible that amphipathic molecules carrying Neu5Gc might be directly transferred into the hESC and hMSC plasma membranes.[19] Human serum contains high titers of natural preformed antibodies against Neu5Gc xenoantigen.[20–22] Thus, binding of these natural preformed antibodies may lead to immune responses such as complement-mediated cytotoxicity (CMC), antibody-dependent cell-mediated cytotoxicity (ADCC), and antibody-dependent cellular phagocytosis. However, these immune responses mediated by natural preformed antibodies against human stem cells remain in controversary.[13,23] This study was therefore undertaken to study the presence of Neu5Gc on hADSCs/MSCs cultured with FBS and the human immune responses mediated by Neu5Gc on hADSCs/MSCs.

Materials and Methods

Cells

hADSCs/MSCs were prepared as described previously[1,2] with modifications.[3,4] Adipose tissue was resected during plastic surgery in five human subjects (four men and one woman; age, 20–60 years) as excess discards. Ten to 50 g of subcutaneous adipose tissue was collected from each subject. All subjects provided informed consent. The protocol was approved by the Review Board for Human Research of the Kobe University Graduate School of Medicine, Osaka University Graduate School of Medicine and Foundation for Biomedical Research and Innovation. All subjects fasted for at least 10 h before surgery and none was being treated with steroids. The resected excess adipose tissue was minced and then digested in Hank's balanced salt solution (Gibco Invitrogen, Grand Island, NY) containing 0.075% collagenase type II (Sigma Aldrich, St. Louis, MO) at 37°C for 1 h. Digests were filtered with a cell strainer (BD Bioscience, San Jose, CA) and centrifuged at 800 *g* for 10 min. Erythrocytes were excluded using density gradient centrifugation with Lymphoprep ($d = 1.077$; Nycomed, Oslo, Norway). The cells were then plated using Dulbecco's modified Eagle's medium (DMEM; Gibco Invitrogen) with 10% defined FBS (Hyclone, Northumberland, United Kingdom) and incubated for 24 h at 37°C. Following incubation, the adherent cells were washed extensively and treated with 0.2 g/L ethylenediaminetetraacetate (EDTA) solution (Nacalai Tesque, Kyoto, Japan), and the resulting suspended cells were replated at a density of 10,000 cells/cm^2 on human fibronectin-coated dishes (BD BioCoat, Franklin Lakes, NJ) in a medium containing 60% DMEM-low glucose, 40% MCDB-201 medium (Sigma Aldrich), 1×insulin–transferrin–selenium (Gibco Invitrogen), 1 nM dexamethasone (Sigma Aldrich), 100 μM ascorbic acid 2-phosphate (Sigma Aldrich), 10 ng/mL epidermal growth factor (PeproTec, Rocky Hill, NJ), and 5% FBS. For analysis of the effects of human serum on Neu5Gc expression on hADSCs/MSCs, the cells were cultured for 7 days, where FBS was replaced by 5% heat-inactivated normal human pooled serum (NHS) from type AB blood. As control cells, a murine pancreatic cell line, Panc02, was cultured with RPMI 1640 medium (Gibco Invitrogen) supplemented with 10% FBS and 1% antibiotic/antimycotic solution.

Flow cytometry

Cells were detached from culture dishes and suspended in Dulbecco's phosphate-buffered saline (D-PBS; Nacalai Tesque). Aliquots (5×10^5 cells) were incubated for 30 min at 4°C with a chicken anti-Neu5Gc polyclonal antibody (a gift from Prof. N. Wakamiya, Asahikawa Medical College, Hokkaido, Japan).[24] Cells incubated with D-PBS alone were used as negative control. After washing with D-PBS, cells were stained with fluorescein isothiocyanate (FITC)-conjugated rabbit anti-chicken immunoglobulin G (IgG; Cappel, Cochranville, PA) as a second antibody. After staining, the cells were washed

FIG. 1. Expression of Neu5Gc on hADSCs/MSCs. (**A**) Specificity of anti-Neu5GC antibody. Panc02, a cell line derived from murine pancreatic carcinomas, expressed Neu5Gc. Flow cytometric analysis showed that chicken anti-Neu5Gc polyclonal antibody bound to the surfaces of Panc02, but Neu5Gc-preadsorbed anti-Neu5Gc polyclonal antibody could not react, showing specificity of the anti-Neu5Gc antibody. The percentage of cells that stained positive is indicated in the upper right corner of each panel. (**B**) Expression of Neu5Gc xenoantigen on hADSCs/MSCs. Fresh hADSCs/MSCs did not express Neu5Gc on their cell surface. In accordance with passage numbers, the population of Neu5Gc-positive cells increased by cultivation with FBS. The percentage of cells that stained positive is indicated in the upper right corner of each panel. (**C**) Reduction of Neu5Gc xenoantigen by chasing cultivation with human serum. After cultivation of hADSCs/MSCs with heat-inactivated NHS but not FBS, the percentages of Neu5Gc-positive cells have decreased in accordance with culture duration. The decrement manners of second passaged hADSCs/MSCs and fifth passaged ones have been in a similar fashion. The percentage of cells that stained positive is indicated in the upper right corner of each panel. Data are representative of four independent experiments. Neu5Gc, *N*-glycolylneuraminic acid; hADSCs/MSCs, human adipose tissue-stromal cells/mesenchymal stem cells; FBS, fetal bovine serum; NHS, normal human pooled serum; IgG, immunoglobulin G; M1, marked positive area 1; FL1, fluorescence1.

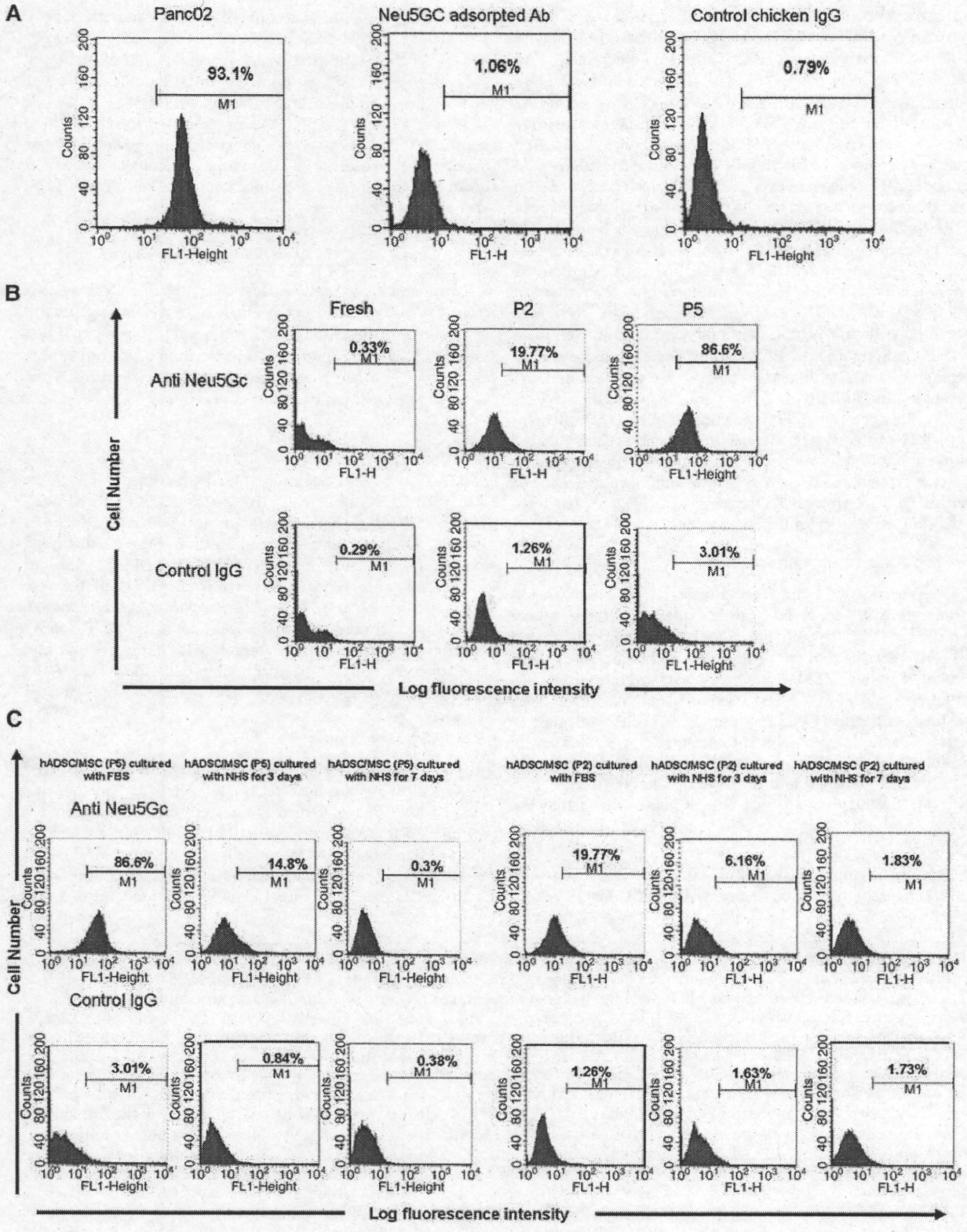
A
Panc02
93.1%
M1
Neu5GC adsorpted Ab
1.06%
M1
Control chicken IgG
0.79%
M1
Counts
FL1-Height
FL1-H
B
Fresh
P2
P5
Anti Neu5Gc
0.33%
19.77%
86.6%
Control IgG
0.29%
1.26%
3.01%
Cell Number
Log fluorescence intensity
C
hADSC/MSC (P5) cultured with FBS
hADSC/MSC (P5) cultured with NHS for 3 days
hADSC/MSC (P5) cultured with NHS for 7 days
hADSC/MSC (P2) cultured with FBS
hADSC/MSC (P2) cultured with NHS for 3 days
hADSC/MSC (P2) cultured with NHS for 7 days
Anti Neu5Gc
86.6%
14.8%
0.3%
19.77%
6.16%
1.83%
Control IgG
3.01%
0.84%
0.38%
1.26%
1.63%
1.73%
Cell Number
Log fluorescence intensity

and resuspended in D-PBS with 150 ng/mL 7-AAD (BD Pharmingen) to eliminate dead cells. The cells were analyzed by flow cytometry using a FACSCalibur flow cytometer and CellQuest Pro software (BD Biosciences, Franklin Lakes, NJ). Data shown in figures are gated for live cells by excluding cells that stained positive for 7-AAD. Percentage of positive cells was defined against a 99% negative control exclusion gate. For detection of binding of human natural preformed antibodies, the cells were exposed to 10% fresh NHS or 5 mM Neu5Gc-preadsorbed NHS in D-PBS containing 15 mM EDTA for 30 min at 4°C. After washing, the cells were stained with FITC-conjugated goat anti-human IgG or IgM antibody (Cappel), or control goat IgG, respectively. To examine the blocking effects of anti-Neu5Gc antibody onto the surface of hADSCs/MSCs, hADSCs/MSCs cultured with FBS were precoated with anti-Neu5Gc antibody, exposed to 10% fresh NHS containing 15 mM EDTA, and then applied for flow cytometric analysis. Stained cells were washed and resuspended in D-PBS with 7-AAD and analyzed by a FACSCalibur flow cytometer. For detection of human complement regulatory proteins, cells were stained with FITC-conjugated mouse monoclonal antibodies to human CD46 (membrane cofactor protein), CD55 (decay accelerating factor), CD59, or control IgG (all from BD Pharmingen) and analyzed by a FACSCalibur flow cytometer as well.

Detection of complement deposition

The amounts of C4 and C3 fragments deposited on the cell surface were also analyzed by flow cytometry. The cells were detached by 0.25% trypsin/EDTA and subsequently incubated with 10% fresh NHS in DMEM for 30 min at 37°C. Cells incubated with DMEM alone or 10% fresh NHS in DMEM containing 15 mM EDTA was used as negative control. After washing with cold D-PBS three times, the cells were stained with FITC-conjugated rabbit anti-human C4c or C3c antibody (Dako, Cambridgeshire, United Kingdom). After staining, the cells were washed and resuspended in 500 μL of D-PBS with 7-AAD and analyzed by a FACSCalibur flow cytometer.

CMC assay

CMC was evaluated by measuring lactate dehydrogenase (LDH) release in media, using MTX-LDH kit (Kyokuto Pharm, Tokyo, Japan) in accordance with the manufacturer's instructions. Target cells (hADSCs/MSCs cultured with FBS, hADSCs/MSCs cultured with heat-inactivated NHS, or Panc02) were plated at a concentration of 1×10^4 cells/well in a 96-well culture plate. Then, DMEM with 20% or 40% fresh NHS was added. The plates were incubated for 2 h at 37°C, and LDH release was determined. All assays included maximal release controls (1% Triton X), controls with medium and target cells, with medium containing fresh NHS, and with medium alone.

Isolation of effector cells

Peripheral blood mononuclear cells (PBMCs) were isolated from the buffy coats from healthy volunteers using density gradient centrifugation with Lymphoprep (Nycomed). Cell viability was more than 98%, as determined by trypan blue exclusion. Human monocyte-derived macrophages were isolated and cultured as reported previously.[25]

ADCC assay

ADCC was also determined by measuring LDH release into medium. Target cells (hADSCs/MSCs cultured with FBS, hADSCs/MSCs cultured with heat-inactivated NHS, or Panc02) were plated in 96-well culture plates as described earlier. Then, 1×10^5 or 2×10^5 PBMCs in DMEM alone or with 10% heat-inactivated NHS were added. The plates were incubated for 4 h at 37°C, and LDH release was determined. All assays included maximal release controls (1% Triton X), controls with medium and target cells, with medium and effector cells, with medium containing 10% heat-inactivated NHS, and with medium alone.

Phagocytosis assay

Target cells (hADSCs/MSCs cultured with FBS, hADSCs/MSCs cultured with heat-inactivated NHS, or Panc02) were stained with PKH67 Green Fluorescent Cell Linker Mini Kit (Sigma Aldrich) according to the manufacturer's instructions. After labeling of target cells was terminated, the cells were washed and resuspended in RPMI medium. Then, 2×10^6 PKH67-labeled target cells were added into 24-well

FIG. 2. Binding of natural preformed antibodies to hADSCs/MSCs. (**A**) Binding of natural preformed antibodies to Panc02 and hADSCs/MSCs. (**a**) Murine pancreatic carcinoma cell line Panc02 was exposed to 10% fresh NHS containing 15 mM EDTA, then stained with secondary FITC-conjugated goat anti-human IgG or IgM antibody, and studied by flow cytometry to demonstrate the binding of IgG and IgM. The natural performed antibodies human IgG and IgM bound onto Panc02. Exposition of Neu5Gc-preadsorbed NHS could reduce the natural performed antibody binding (IgG binding: 99.95% to 85.09%; IgM binding: 92.8% to 44.49%). (**b**) hADSCs/MSCs were cultured with FBS, exposed to 10% fresh NHS containing 15 mM EDTA, and then stained with secondary FITC-conjugated goat anti-human IgG or IgM antibody, or control goat IgG. The natural performed antibodies human IgG and IgM bound onto hADSCs/MSCs, and exposition of Neu5Gc-preadsorbed NHS could reduce IgG binding (80.01% to 2.08%). The percentage of cells that stained positive is indicated in the upper right corner of each panel. Data are representative of four independent experiments. (**B**) Anti-Neu5Gc antibody pretreatment suppressed the binding of natural preformed antibodies onto hADSCs/MSCs. hADSCs/MSCs cultured with FBS were precoated with anti-Neu5Gc antibody and then exposed to 10% fresh NHS containing 15 mM EDTA. The natural performed antibody human IgG bound onto hADSCs/MSCs, and exposition of anti-Neu5Gc antibody could reduce IgG binding (70.33% to 1.74%). The percentage of cells that stained positive is indicated in the upper right corner of each panel. Data are representative of three independent experiments. (**C**) Decrement of binding of natural preformed antibodies onto hADSCs/MSCs by chase with NHS. After cultivation of hADSCs/MSCs with heat-inactivated NHS but not FBS, the percentages of human IgG-positive cells decreased. The percentage of cells that stained positive is indicated in the upper right corner of each panel. Data are representative of four independent experiments. hADMSCs, adipose-tissue derived mesenchymal stem cells; EDTA, ethylenediaminetetraacetate; FITC, fluorescein isothiocyanate.

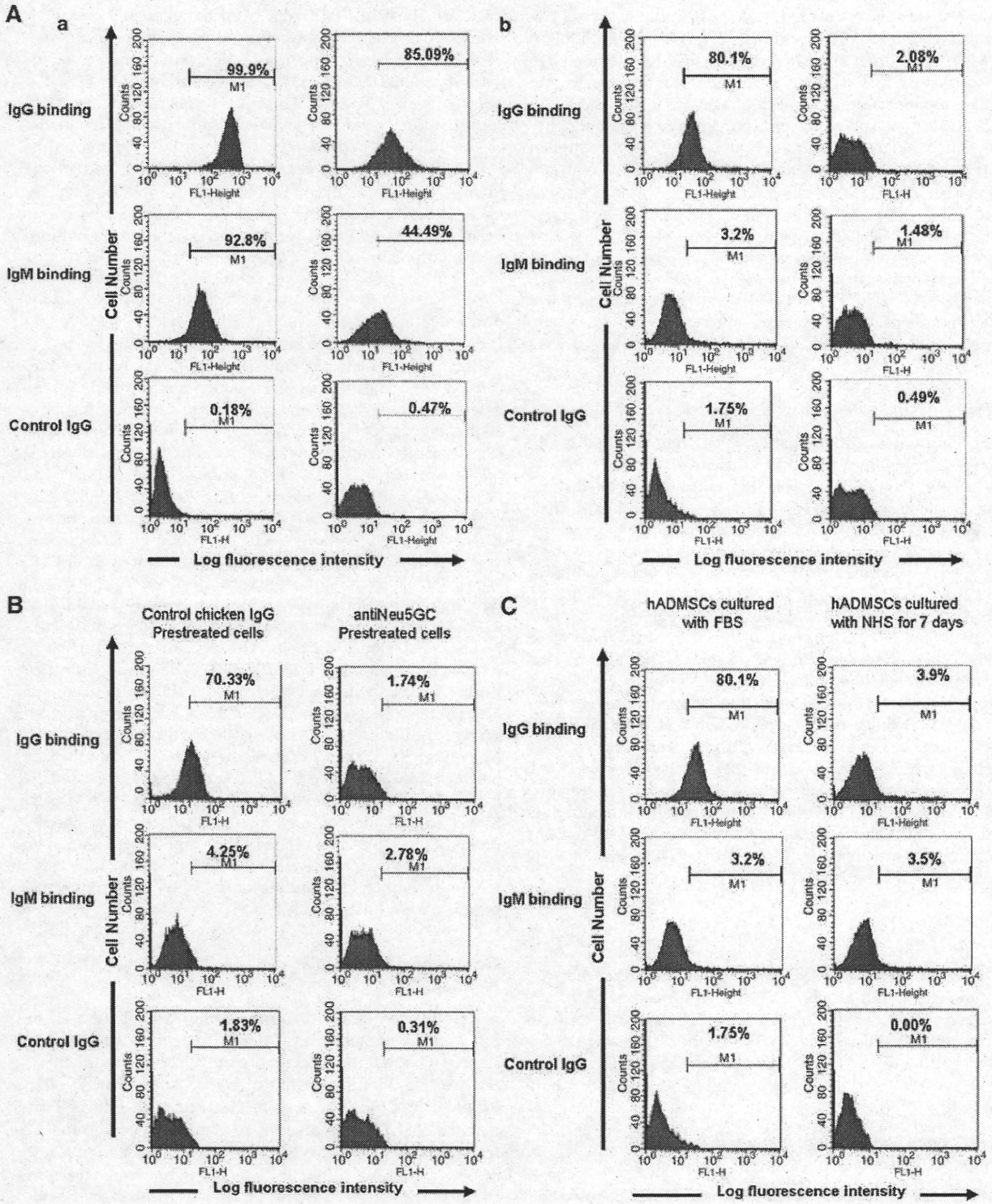
A
a
b
IgG binding
IgM binding
Control IgG
99.9%
85.09%
92.8%
44.49%
0.18%
0.47%
80.1%
2.08%
3.2%
1.48%
1.75%
0.49%
M1
Counts
FL1-Height
FL1-H
Cell Number
Log fluorescence intensity
B
Control chicken IgG
Prestreated cells
antiNeu5GC
Prestreated cells
70.33%
1.74%
4.25%
2.78%
1.83%
0.31%
C
hADMSCs cultured
with FBS
hADMSCs cultured
with NHS for 7 days
80.1%
3.9%
3.2%
3.5%
1.75%
0.00%

culture plates and incubated with 2×10^5 human monocyte-derived macrophages (Effector:Target [*E*:*T*] = 1:10) in 1 mL of RPMI 1640 medium alone or with 10% heat-inactivated NHS for 24 h at 37°C. Following incubation, the target cells and human monocyte-derived macrophages were harvested with EDTA solution. The cells were counterstained with allophycocyanin-conjugated mouse monoclonal antibodies to human CD11c (BD Pharmingen) and washed and fixed with 2% formaldehyde-PBS. Two-color flow cytometric analysis was performed with a FACSCalibur flow cytometer under optimal gating. PKH67-labeled target cells were detected in the FL-1 channel and allophycocyanin-labeled human monocyte-derived macrophages were detected in the FL-4 channel. Dual-labeled cells ($PKH67^+/CD11c^+$) were considered to represent phagocytosis of targets by human monocyte-derived macrophages. Residual target cells were defined as cells that were $PKH67^+/CD11c^+$.

Adipogenic and osteogenic differentiation procedure

For adipogenic differentiation, cells were cultured in differentiation medium (Zen-Bio, Durham, NC). After 3 days, half of the medium was changed with adipocyte medium (Zen-Bio) every 2 days. Ten days after differentiation, characterization of adipocytes was confirmed by microscopic observation of intracellular lipid droplets by oil red O staining. Osteogenic differentiation was induced by culturing the cells in DMEM containing 10 nM dexamethasone, 50 mg/dL ascorbic acid 2-phosphate, 10 mM beta-glycerophosphate (Sigma, St. Louis, MO), and 10% FBS or heat-inactivated NHS. The differentiation was examined by alizarin red staining and alkaline phosphatase (AP) activity. For alizarin red staining, 7 or 18 days after differentiation, the cells were washed three times and fixed with dehydrated ethanol. After fixation, the cells were stained with 1% alizarin red S in 0.1% NH_4OH (pH 6.5) for 5 min and then washed with H_2O. AP activity was investigated at 2 weeks after differentiation using the procedure described previously.[26] AP activity per cell was calculated based on the amount of DNA. DNA content was measured by a modification of the method of Labarca and Paigen.[27]

Statistics

Values are given as the mean ± standard deviation. Student's *t*-test was used to ascertain the significance of differences within groups. Differences were considered statistically significant when $p < 0.05$. All statistical analyses were performed using the SPSS Statistics 17.0 package (SPSS, Chicago, IL).

Results

Presence of Neu5Gc and human natural preformed antibodies binding to hADSCs/MSCs

First, the specificity of chicken anti-Neu5Gc polyclonal antibody was examined (Fig. 1A). Flow cytometric analysis showed that chicken anti-Neu5Gc polyclonal antibody bound to the surfaces of Panc02, which constitutively expressed Neu5Gc, but Neu5Gc-preadsorbed anti-Neu5Gc polyclonal antibody could not react, indicating the anti-Neu5Gc antibody reacts to Neu5Gc specifically. Next, incorporation of Neu5Gc antigen via FBS-containing medium was examined (Fig. 1B). Fresh hADSCs/MSCs did not express Neu5Gc on their cell surface. In accordance with passage numbers, the population of Neu5Gc-positive cells has increased by cultivation with FBS (fresh: 0.33%; passage number 2: 19.77%; and passage number 5: 86.6%). Culture with heat-inactivated NHS could markedly reduce Neu5Gc in human colon carcinoma cells,[22] hESCs,[13] and hMSCs,[14] apparently as the result of metabolic replacement by *N*-acetylneuraminic acid in the human serum. So, the reduction of incorporated Neu5Gc xenoantigen by chasing cultivation with human serum was examined (Fig. 1C). The Neu5Gc xenoantigen was reduced after cultivation of hADSCs/MSCs with heat-inactivated NHS but not FBS. The percentages of Neu5Gc-positive cells have decreased in accordance with culture duration, and the decrement manners of second passaged hADSCs/MSCs and fifth passaged ones have been in a similar fashion.

Because human serum contains high titers of natural preformed antibodies against the Neu5Gc xenoantigen,[20–22] we assessed whether such antibodies could recognize Neu5Gc-containing epitopes on hADSCs/MSCs cultured with FBS (Fig. 2). Panc02 cultured with FBS and exposed to 10% fresh NHS containing 15 mM EDTA showed high human IgG (99.9%) and IgM (92.8%) binding (Fig. 2Aa). hADSCs/MSCs cultured with FBS and treated with fresh NHS also showed high human IgG binding (80.1%), but human IgM binding was very low (3.2%) (Fig. 2Ab). Preincubation of fresh NHS with Neu5Gc resulted in significant decrease in human IgG binding on hADSCs/MSCs cultured with FBS (80.1% to 2.08%). Further, pretreatment of hADSCs/MSCs with anti-Neu5Gc polyclonal antibody also resulted in reduction of human IgG binding (70.33% to 1.74%; Fig. 2B). Culturing hADSCs/MSCs with heat-inactivated NHS, which decreased Neu5Gc expression of hADSCs/MSCs effectively, reduced human IgG binding on hADSCs/MSCs when exposed to fresh NHS (Fig. 2C). Taken together, these data indicate that the hADSCs/MSCs cultured with FBS expressed Neu5Gc and the human natural preformed antibodies could bind to hADSCs/MSCs. This binding of human natural preformed antibodies on hADSCs/MSCs was related to the amount of Neu5Gc on hADSCs/MSCs. Culture with heat-inactivated NHS could markedly reduce IgG binding on hADSCs/MSCs when exposed to fresh NHS (80.1% to 3.9%).

Complement fragment deposition on hADSCs/MSCs and CMC assay

Cell surface antibody binding may activate the classical complement pathway leading to cytotoxicity. We assessed whether the deposition of complement fragments on hADSCs/MSCs occurred after exposure to fresh NHS. Whether hADSCs/MSCs were cultured with FBS or heat-inactivated NHS, the amount of deposition of C4 and C3 fragments on hADSCs/MSCs after a short incubation period of 30 min was no different from negative control (cells incubated with DMEM alone or 10% fresh NHS in DMEM containing 15 mM EDTA) (Fig. 3). To control for fresh NHS activity and variability, we tested the deposition of C4 and C3 fragments on Panc02. Both complement fragments were clearly deposited on Panc02 (C4: 84.6%; C3: 98.99%) and this deposition was abolished by adding 15% EDTA (Fig. 3). We next analyzed the CMC of hADSCs/MSCs cultured with FBS or heat-inactivated NHS. To control for CMC of fresh NHS,

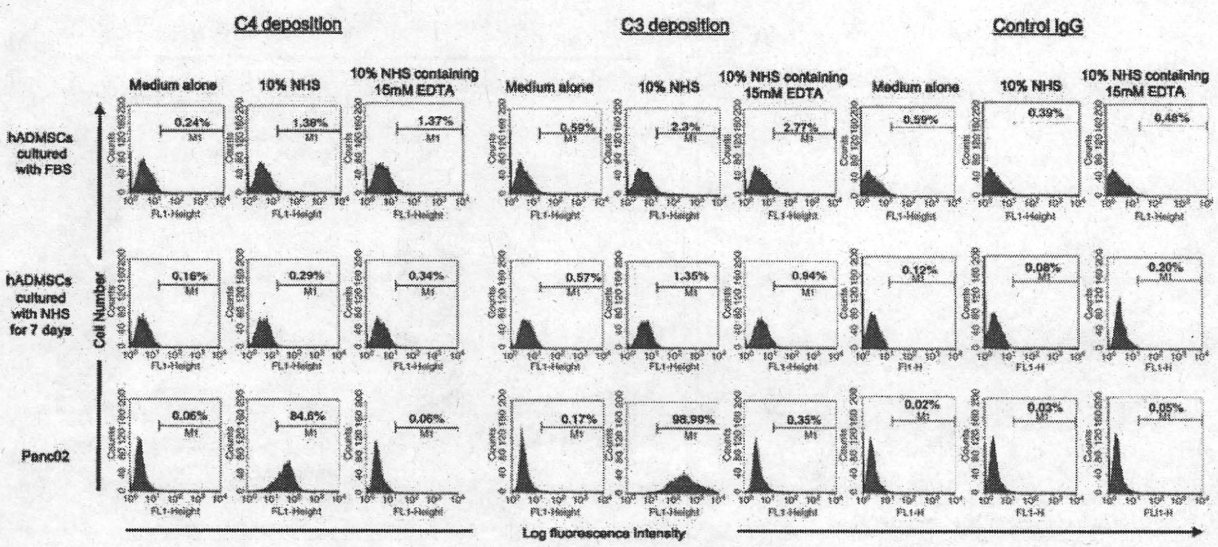

FIG. 3. Complement deposition onto hADSCs/MSCs by NHS. The cells were exposed to medium alone, 10% NHS, or 10% NHS containing 15 mM EDTA, followed by an analysis of deposition of complement fragments C4 and C3. The percentage of cells that stained positive is indicated in the upper right corner of each panel. Data are representative of four independent experiments.

we tested CMC of Panc02. CMC of Panc02 was clearly detected (20% NHS: 42.7% ± 4.7%; 40% NHS: 65.4% ± 2.4%). In contrast, significant specific lysis of hADSCs/MSCs cultured with FBS or heat-inactivated NHS was not detected (hADSCs/MSCs cultured with FBS + 20% NHS: 4.8% ± 1.3%; or 40% NHS: 7.4% ± 2.0%; hADSCs/MSCs cultured with heat-inactivated NHS: 20% NHS: 3.6% ± 1.6%; 40% NHS: 5.6% ± 1.6%). We then analyzed the expression of complement regulatory proteins such as CD46, CD55, and CD59 on hADSCs/MSCs. hADSCs/MSCs were weakly positive for both CD46 (22.1%) and CD55 (29.8%) and highly positive for CD59 (97.5%) (Fig. 4B). These data indicate that hADSCs/MSCs express complement regulatory proteins such as CD46, CD55, and CD59 and are largely resistant to killing by CMC mechanism.

ADCC of hADSCs/MSCs mediated by human natural preformed antibodies in NHS

IgG antibodies play an important role in ADCC.[28] Our study demonstrated that natural preformed IgG antibodies could bind to hADSCs/MSCs cultured with FBS. Therefore, to evaluate the role of these IgG antibodies in cell-mediated cytotoxicity, ADCC assay was performed with hADSCs/MSCs cultured with FBS, hADSCs/MSCs cultured with heat-inactivated NHS, or Panc02 as targets and human PBMCs as effector cells, using *E:T* ratios of 10:1 and 20:1, and 4-h incubation periods. PBMCs in the absence of heat-inactivated NHS caused no significant lysis of hADSCs/MSCs cultured with FBS, hADSCs/MSCs cultured with heat-inactivated NHS, and Panc02 (hADSCs/MSCs cultured with FBS: *E:T* = 10:1, 2.37% ± 0.35%; *E:T* = 20:1, 3.78% ± 0.85%; hADSCs/MSCs cultured with heat-inactivated NHS: *E:T* = 10:1, 0.57% ± 0.36%; *E:T* = 20:1, 2.34% ± 0.67%; Panc02: *E:T* = 10:1, 1.98% ± 0.35%; *E:T* = 20:1, 4.7% ± 0.54; Fig. 5, white bar). The cytotoxicity of Panc02 in the presence of heat-inactivated NHS was significantly greater than that in the absence of heat-inactivated NHS (in the presence of NHS vs. in the absence of heat-inactivated NHS: *E:T* = 10:1, 27.4% ± 3.1% vs. 1.98% ± 0.35%, $p < 0.05$; *E:T* = 20:1, 28.9% ± 4.6% vs. 4.7 ± 0.54%, $p < 0.05$), which proved the effective use of PBMCs (Fig. 5). A significant increase of cytotoxicity of the hADSCs/MSCs cultured with FBS was also evident in the presence of heat-inactivated NHS (in the presence of heat-inactivated NHS vs. in the absence of heat-inactivated NHS: *E:T* = 10:1, 13.5% ± 0.82% vs. 2.37% ± 0.35%, $p < 0.05$; *E:T* = 20:1, 16.0% ± 1.5% vs. 3.78% ± 0.85, $p < 0.05$; Fig. 5). In contrast, no increase of cytotoxicity of the hADSCs/MSCs cultured with heat-inactivated NHS was detected in the presence of heat-inactivated NHS (in the presence of heat-inactivated NHS vs. in the absence of heat-inactivated NHS: *E:T* = 10:1, 3.23% ± 0.52% vs. 0.57% ± 0.36%; *E:T* = 20:1, 3.75% ± 0.51% vs. 2.34% ± 0.67%; Fig. 5). In addition, the cytotoxicity the hADSCs/MSCs cultured with FBS was significantly greater than that of hADSCs/MSCs cultured with heat-inactivated NHS which expressed negligible amount of Neu5Gc (hADSCs/MSCs cultured with FBS vs. hADSCs/MSCs cultured with heat-inactivated NHS: *E:T* = 10:1, 13.5% ± 0.82% vs. 3.23% ± 0.52%, $p < 0.05$; *E:T* = 20:1, 16.0% ± 1.5% vs. 3.75% ± 0.51, $p < 0.05$; Fig. 5). Taken together, these data indicate that the hADSCs/MSCs cultured with FBS are injured by ADCC mechanism. In contrast, hADSCs/MSCs cultured with NHS are less sensitive to ADCC.

Phagocytosis of hADSCs/MSCs by human monocyte-derived macrophages

hADSCs/MSCs cultured with FBS, hADSCs/MSCs cultured with heat-inactivated NHS, or Panc02 were stained with fluorescent PKH67, respectively. Labeled cells were cocultured with human monocyte-derived macrophages in the presence or absence of heat-inactivated NHS for 24 h. After counterstaining with monoclonal antibodies to human CD11c, two-color flow cytometric analysis was performed

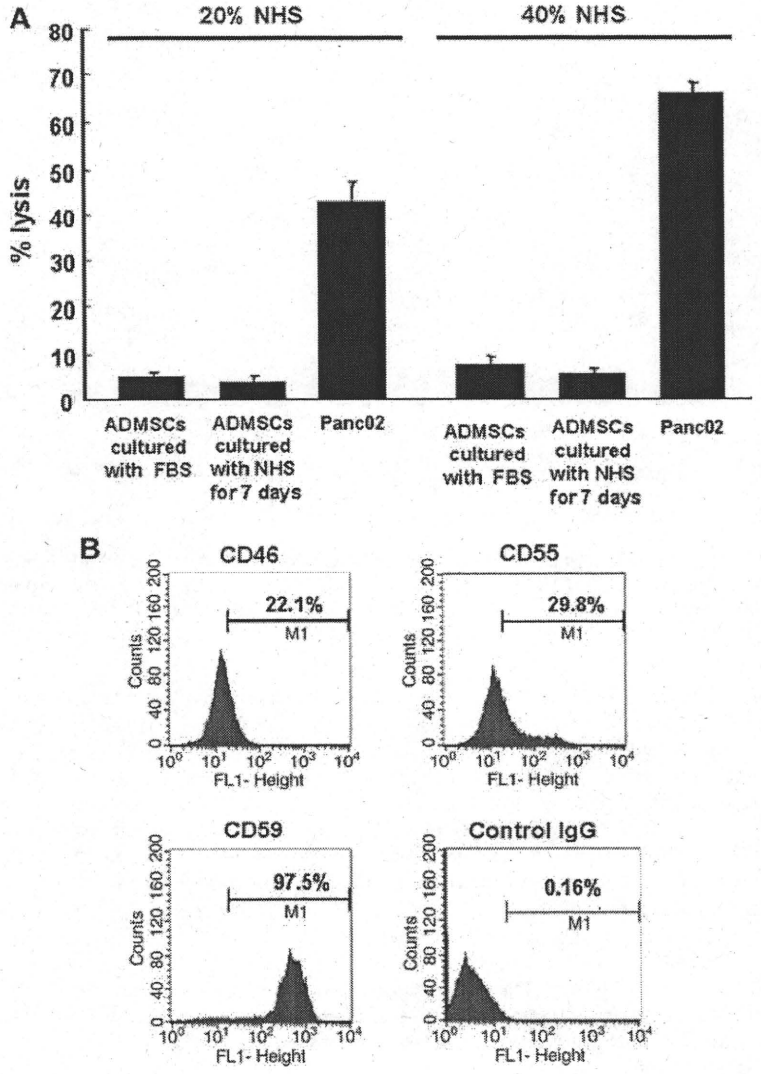

FIG. 4. Sensitivity of hADMSCs to lysis by NHS. (**A**) Complement-mediated cytotoxicity assay of hADSCs/MSCs. The cytotoxic activity of 20% or 40% NHS against hADSCs/MSCs was tested by lactate dehydrogenase release. Data are shown as mean ± standard deviation. (**B**) Complement regulatory proteins on hADSCs/MSCs were studied by flow cytometry using FITC-conjugated antibodies to human CD46, CD55, CD59, or control IgG. Data are representative of three independent experiments.

(Fig. 6). Phagocytosis of target cells by human monocyte-derived macrophages could be identified as dual-labeled cells ($PKH67^+/CD11c^+$, right upper panel). Similar results were obtained in three independent experiments. Phagocytosis of Panc02 was clearly detectable (10.6%) and increased twofold in the presence of heat-inactivated NHS, which proved the effective use of human monocyte-derived macrophages. Phagocytosis of hADSCs/MSCs cultured with NHS by human monocyte-derived macrophages was somewhat detectable (5.7%) and also increased in the presence of heat inactivated human serum (9.3%). In contrast, human monocyte-derived macrophages could not phagocytose hADSCs/MSCs cultured with heat-inactivated NHS neither in the absence nor in the presence of heat-inactivated NHS (medium alone: 1.1%; 10% heat-inactivated NHS: 2.2%; Fig. 6). Thus, human monocyte-derived macrophages phagocytosed hADSCs/MSCs cultured with FBS and this phagocytic activity increased when hADSCs/MSCs cultured with FBS were opsonized by the natural preformed antibodies in the presence of heat-inactivated NHS. In contrast, hADSCs/MSCs cultured with heat-inactivated NHS were resistant to phagocytosis either in the absence or in the presence of heat-inactivated NHS.

Adipogenic and osteogenic differentiation potentials of hADSCs/MSCs cultured with FBS and heat-inactivated NHS

To compare the *in vitro* differentiation potential of hADSCs/MSCs cultured with FBS or heat-inactivated NHS, cells were differentiated toward the adipogenic and osteogenic lineages. Adipogenic differentiation was induced by culture with differentiation medium containing 1-methyl-3-isobutylxanthine, peroxisome proliferator-activated receptor (PPAR)-gamma agonist, dexamethasone, and insulin. The acquisition of the adipogenic phenotype was determined by staining the cell monolayers with oil red O (Fig. 7A). The efficiency of adipogenesis of hADSCs/MSCs cultured with heat-inactivated NHS was similar to that of hADSCs/MSCs cultured with FBS (Fig. 7A). Both hADSCs/MSCs showed multiple intracellular lipid-

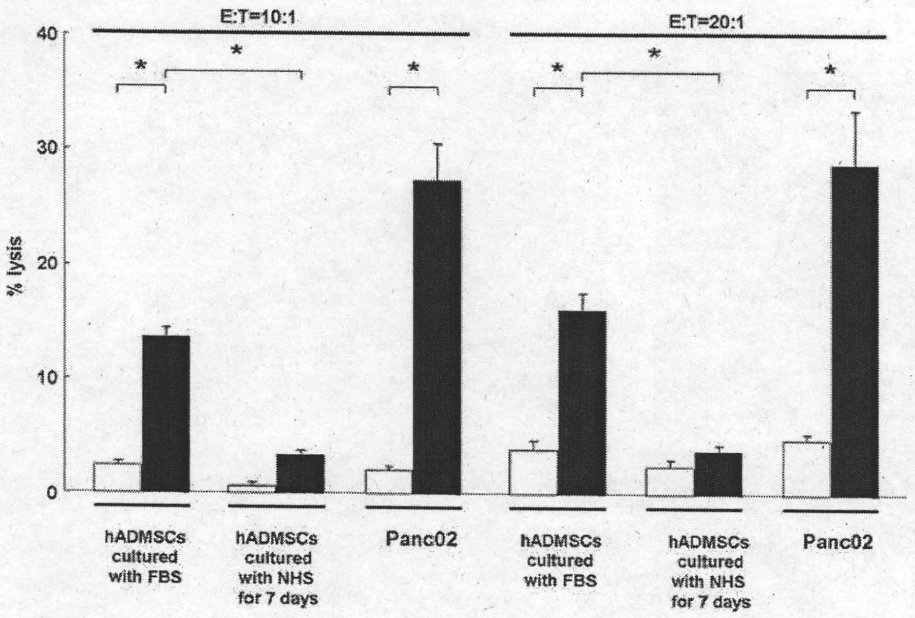

FIG. 5. Antibody-dependent cell-mediated cytotoxicity assay of hADSCs/MSCs. The cytotoxic activity of peripheral blood mononuclear cells against hADSCs/MSCs in the absence (white bar) or presence (black bar) of 10% NHS was tested by measuring lactate dehydrogenase release into medium (Effector:Target [*E:T*] = 10:1 or 20:1). Data are shown as mean ± standard deviation ($^*p < 0.05$) and are representative of three independent experiments.

filled droplets in 35–50% of cells after adipogenic induction. Osteogenic differentiation was induced by treating cells with low concentrations of dexamethasone, ascorbic acid, and beta-glycerophosphate. Calcium deposition was demonstrated by staining monolayers with alizarin red (Fig. 7B). hADSCs/MSCs cultured with heat-inactivated NHS and those cultured with FBS showed similar potential toward osteogenic differentiation. High AP activity was detected in hADSCs/MSCs cultured with heat-inactivated NHS and those cultured with FBS in response to osteogenic induction after 2 weeks (Fig. 7B).

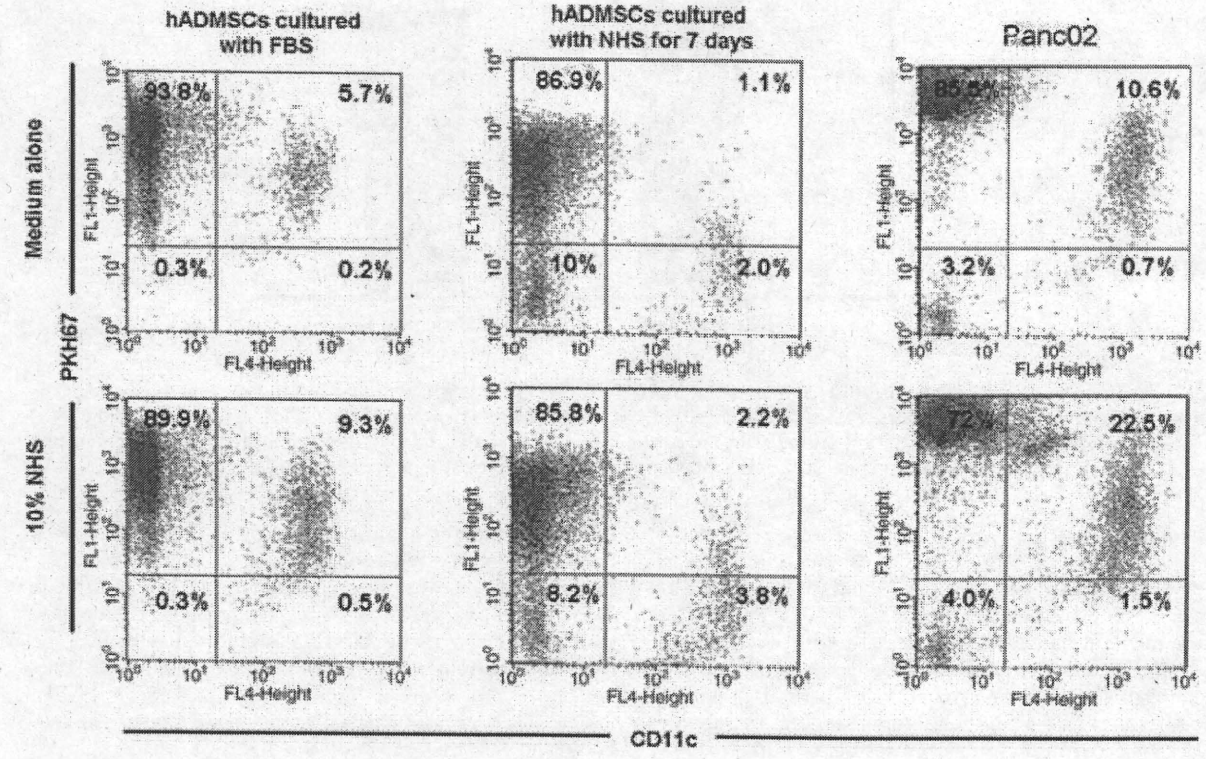

FIG. 6. Representative flow cytometry profiles of phagocytosis assay of hADSCs/MSCs. Upper left quadrant: Region of residual target cells. Upper right quadrant: Region of phagocytosed target cells. Percentages represent those of total cells in each region. Data are representative of three independent experiments.

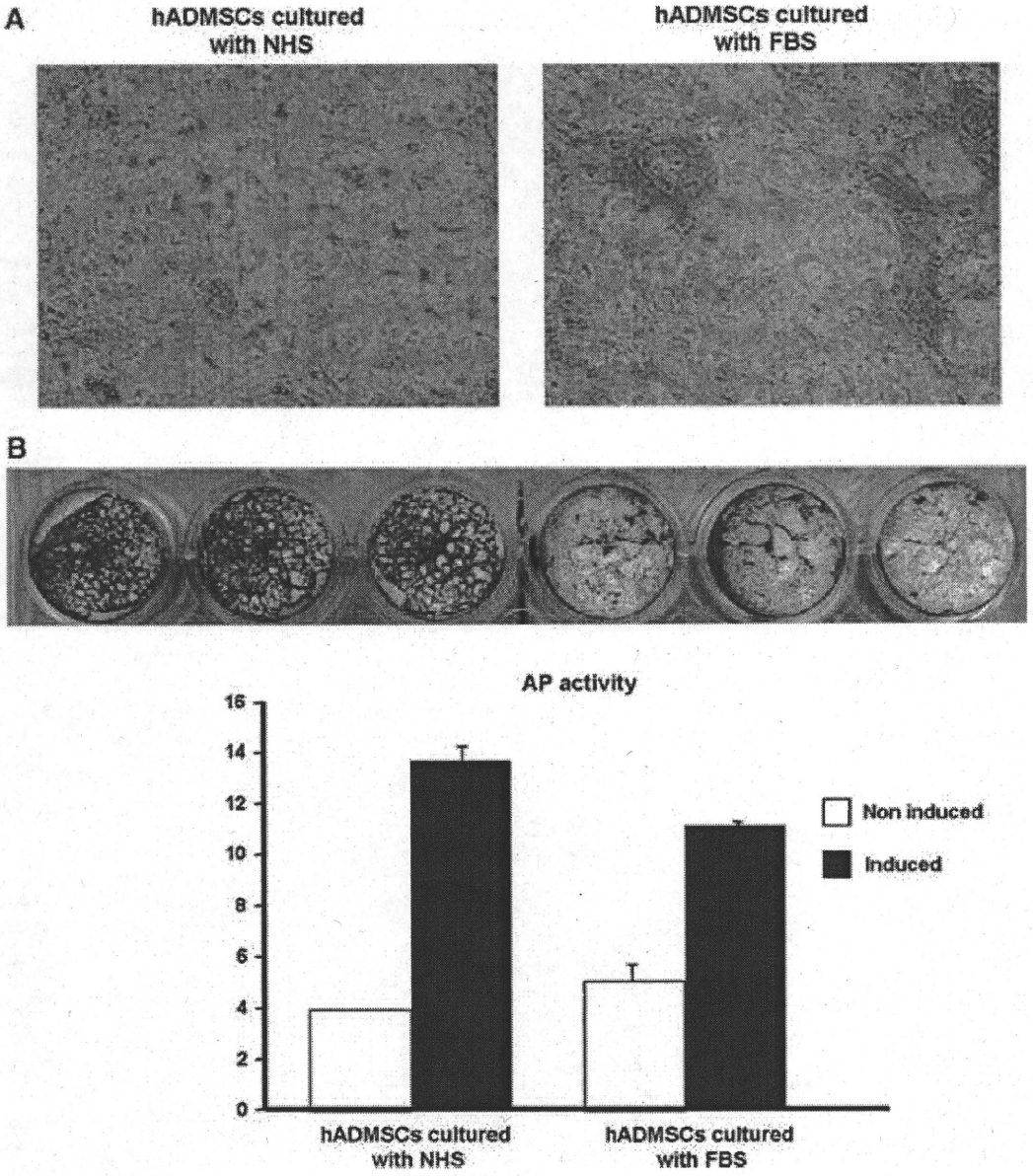

FIG. 7. Adipogenic and osteogenic differentiation potentials of hADSCs/MSCs cultured with FBS and NHS. (**A**) The efficiency of adipogenesis of hADSCs/MSCs cultured with NHS was similar to that of hADSCs/MSCs cultured with FBS. (**B**) The efficacy of osteogenic differentiation and alkaline phosphatase activity was similar between cultures with NHS and FBS in response to osteogenic induction. Data are representative of four independent experiments.

Discussion

Previous studies have reported that hESCs and BM-derived hMSCs are capable of efficient Neu5Gc uptake from culture media components.[13,14] Human serum contains high titers of natural preformed antibodies against Neu5Gc xenoantigen[20–22] and binding of these natural preformed antibodies may lead to immune responses. Importantly, this may be reflected in the published results of human clinical trials using BM-derived hMSCs cultured with FBS.[8–12] Further, in human clinical trials with FBS-grown hMSCs, antibodies against FBS have been detected.[12] However, these immune responses against human stem cells mediated by natural preformed antibodies remain in controversary.[13,23] In this study, because of the usefulness of hADSCs/MSCs as an alternative source of stem cells, we assessed the presence of Neu5Gc in hADSCs/MSCs cultured with FBS and the human immune response mediated by Neu5Gc xenoantigen.

Our study using a chicken anti-Neu5Gc polyclonal antibody showed that most of the hADSCs/MSCs cultured with FBS expressed Neu5Gc xenoantigen. This result is similar to the previous study that hESCs and BM-derived hMSCs express Neu5Gc.[13,14] In addition, our data suggested

that human natural preformed antibodies could bind to hADSCs/MSCs after exposure to fresh NHS. The subtype of natural preformed antibodies was mainly IgG, not IgM. This human IgG binding was related to the amount of Neu5Gc on the hADSCs/MSCs, because hADSCs/MSCs cultured with heat-inactivated NHS which expressed negligible levels of Neu5Gc showed negligible levels of IgG binding when exposed to fresh NHS. This result is also consistent with the previous study that anti-Neu5Gc antibodies constitute the majority of natural preformed xenoreactive antibodies besides anti-galactose-alpha 1,3-galactose (Gal) antibodies, particularly in the IgG subclass.[20,29] In effect, hADSCs/MSCs cultured with FBS may seem like xenogeneic cells to the human immune systems.

When xenogeneic grafts are transplanted into humans, binding of natural preformed antibodies that recognize xenoantigens, including Gal and Neu5Gc, mediates two types of rejection response, hyperacute rejection (HAR) and acute humoral xenograft rejection (AHXR).[30] HAR begins with binding of natural preformed antibodies to the xenogeneic epitopes on donor endothelial cells, including Gal and Neu5Gc xenoantigens, leading to complement activation by mainly classical pathway.[30] The graft is rejected within minutes to hours. Therefore, we analyzed the CMC of hADSCs/MSCs cultured with FBS that express Neu5Gc xenoantigen, using fresh NHS. However, we could not confirm the existence of CMC. The deposition of C4 and C3 fragments on hADSCs/MSCs after a short incubation with fresh NHS could not also be detected. In this issue, there are no reports describing the CMC of hADSCs/MSCs cultured with FBS that express Neu5Gc xenoantigen. Martin *et al.* reported that binding of natural preformed antibodies to Neu5Gc on hESCs mediated complement activation leading to cell death.[13] In contrast, Cerdan *et al.* reported that complement activation by anti-Neu5Gc antibody does not mediate killing of hESCs.[23] Several reasons for this discrepancy have been supposed. One is the difference of procedures used for testing cell cytotoxicity. Previous two reports detected cell cytotoxicity by propidium iodide or 7-AAD exclusion using flow cytometry. Single-cell suspension required for this procedure may cause extensive cell death even under controlled conditions. We detected cell cytotoxicity by conventional LDH release assay, which is often used in cytotoxicity assays.[32,33] The other and more possible reason is the biological difference among the human stem cells, including hESCs and hMSCs. We assessed the expression of complement regulatory proteins such as CD46, CD55, and CD59 on hADSCs/MSCs. hADSCs/MSCs were weakly positive for both CD46 and CD55 and highly positive for CD59. It is reported that HAR could be prevented by inhibiting complement activation, using transgenic animals bearing transgenes encoding human complement regulatory proteins.[34–36] Thus, it is supported that hADSCs/MSCs express complement regulatory proteins and may be largely resistant to killing by CMC mechanism. However, the expression of complement regulatory proteins on other human stem cells such as hESCs remains uncertain and further investigation is needed.

AHXR occurs when HAR is prevented, and it can be induced by low levels of natural preformed antibodies.[30] The binding of natural preformed antibodies to xenogeneic endothelial cells results in ADCC by natural killer cells, macrophages, and neutrophils, endothelial cell activation, thrombosis, and vasoconstriction.[30] It is reported that AHXR could be mediated by natural preformed antibodies against non-Gal xenoantigen,[37,38] particularly Neu5Gc xenoantigen.[39] Therefore, we analyzed the ADCC of hADSCs/MSCs cultured with FBS that express Neu5Gc xenoantigen. Our data indicated the clear existence of ADCC of hADSCs/MSCs cultured with FBS. This ADCC is supposed to be mediated by preformed natural antibodies that recognize Neu5Gc because ADCC of hADSCs/MSCs cultured with heat-inactivated NHS which expressed negligible levels of Neu5Gc could not be detected. We also analyzed the antibody-mediated cell phagocytosis of hADSCs/MSCs cultured with FBS by monocyte-derived macrophage because macrophages can target opsonized cells. However, in our study, a low level of phagocytic activity of hADSCs/MSCs cultured with FBS even in the absence of NHS was detected and this phagocytic activity clearly increased in the presence of NHS. Ide *et al.* reported that human macrophages could phagocytose porcine cells in an antibody- and complement-independent manner and elimination of Gal on porcine cells that expressed Neu5Gc did not prevent this phagocytic activity.[40] Our data indicated that hADSCs/MSCs cultured with heat-inactivated NHS which expressed negligible levels of Neu5Gc were resistant to phagocytosis mediated by human macrophages in the presence or absence of fresh NHS. Accordingly, human macrophages may be able to recognize Neu5Gc xenoantigen and phagocytose hADSCs/MSCs.

We showed here that hADSCs/MSCs cultured with FBS expressed Neu5Gc xenoantigen and that binding of natural preformed antibodies led to immune response. Based on current data, it is clear that hADSCs/MSCs should be chased without animal materials. Yamaguchi *et al.* have tried xeno-free techniques on hematopoietic stem cells by growing them on human stromal cells and using medium containing NHS.[41] To eliminate Neu5Gc on hADSCs/MSCs, we cultured them in a medium in which FBS was replaced by heat-inactivated NHS for a week after culturing with FBS. The expression of Neu5Gc on these hADSCs/MSCs was extremely reduced. Heiskanen *et al.* described that BM-derived hMSCs became decontaminated after 2 weeks of culture in a medium in which FBS was replaced by NHS, but complete decontamination was difficult to achieve by changing culture conditions.[14] Therefore, hADSCs/MSCs may not be completely decontaminated with Neu5Gc by culturing with heat-inactivated NHS for a week. However, our data suggested that human immune responses mediated by Neu5Gc on hADSCs/MSCs, such as ADCC and phagocytosis, were nearly completely prevented by this culture condition. Adipogenic and osteogenic differentiation potentials of hADSCs/MSCs cultured with heat-inactivated NHS were not less than that of those cultured with FBS. This work implies that the culture conditions avoiding renewed exposure to animal materials can reduce the expression of Neu5Gc on hADSCs/MSCs and consequently prevent human immune responses against hADSCs/MSCs. Although major complications have not been reported in the clinical trials with hMSCs cultured with FBS, human immune responses mediated by Neu5Gc may potentially influence the survival and efficacy of the transplanted cells and thus bias the published results. For clinical application of stem cell therapies based on hADSCs/MSCs, hADSCs/MSCs that presented Neu5Gc on their cell surfaces after